Semiannual Progress Report

For Stimul-Responsive Polymers with Enhanced Efficiency in Reservoir Recovery Processes

For the work performed during the period of

September 1, 2002 through February 28, 2003

by

Charles McCormick

and

Roger Hester

Issued on March 13, 2003

DOE Award Number DE-FC26-01BC15317

The University of Southern Mississippi
Department of Polymer Science
P.O. Box 10076
Hattiesburg, MS 39406

TABLE OF CONTENTS

FIGURES AND TABLES

Disclaimer

Abstract

Acrylamide-based hydrophobically modified (HM) polybetaines containing *N*-butylphenylacrylamide (BPAM) and varying amounts of either sulfobetaine (3-(2-acrylamido-2-methylpropanedimethylammonio)-1-propanesulfonate, AMPDAPS) or carboxybetaine (4-(2-acrylamido-2-methylpropyldimethylammonio) butanoate, AMPDAB) comonomers were synthesized via micellar copolymerization. The terpolymers were characterized via ^{13}C NMR and UV spectroscopies, classical and dynamic light scattering, and potentiometric titration. The response of aqueous polymer solutions to various external stimuli, including changes in solution pH, electrolyte concentration, and the addition of small molecule surfactants, was investigated using surface tension and rheological measurements. Low charge density terpolymers were found to show greater viscosity enhancement upon the addition of surfactant compared to the high charge density terpolymers. The addition of sodium dodecyl sulfate (SDS) produced the largest maximum in solution viscosity, while *N*-dodecyl-*N*,*N*,*N*-trimethylammonium bromide (DTAB), *N*-dodecyl-*N*,*N*-dimethylammonio-1-propanesulfonate (SB3-12), and Triton X-100 tended to show reduced viscosity enhancement. In most cases, the high charge density carboxybetaine terpolymer exhibited diminished solution viscosities upon surfactant addition.

In our last report, we discussed solution thermodynamic theory that described changes in polymer coil conformation as a function of solution temperature and polymer molecular weight.[01] These polymers contained no ionic charges. In this report, we expand polymer solution theory to account for the electrostatic interactions present in solutions of charged polymers. Polymers with ionic charges are referred to as polyions or polyelectrolytes.

EXECUTIVE SUMMARY

To date, our synthetic research efforts have been focused on the development of stimuli-responsive water-soluble polymers designed for use in enhanced oil recovery (EOR) applications. These model systems are structurally tailored for potential application as viscosifiers and/or mobility control agents for secondary and tertiary EOR methods. The goal of previous synthetic work has been to design novel polymers that exhibit large dilute solution viscosities in the presence of the adverse conditions normally encountered in oil reservoirs (such as high salt concentrations, the presence of multivalent ions, and elevated temperatures). The polymers are also designed to have "triggerable" properties that can be elicited by external stimuli, such as changes in pH and/or salt concentration.

Previously, we have investigated polyzwitterions (i.e. polyampholytes and polybetaines) and hydrophobically modified polyelectrolytes as potential viscosifiers for EOR applications. The polyzwitterions demonstrate remarkable salt tolerance due to their amphoteric nature, while the hydrophobically modified (HM) polyelectrolytes exhibit improved viscosification as a result of intermolecular hydrophobic association, which imparts an additional viscosification mechanism to the polymers. This current research is focused on combining the benefits of polyzwitterions and hydrophobic modification in the same polymer system. Ideally, the HM polyzwitterions will exhibit a unique combination of the stimuli-responsive behaviors observed in previously examined systems.

Another goal of this research is to investigate the interaction of surfactants with the HM polyzwitterions. Surfactants are critical components in micellar enhanced EOR (e.g. polymer-surfactant flooding) processes because of their ability to reduce interfacial tension and mobilize oil trapped in reservoir formations. We aim to synthesize polymer systems that will demonstrate synergistic increases in solution viscosity upon the addition of surfactants. Such polymer systems may demonstrate superior performance as mobility control agents in micellar enhanced EOR processes due to surfactant-induced viscosity enhancement.

Experience has shown that efficient polymers for oil recovery must have a large hydrodynamic coil size in solution as they flow through the reservoir. Larger polymer coils have higher extensional viscosities, which lower aqueous phase mobility in the porous media, and thereby improve sweep efficiency to displace residual reservoir oil. Ideally, the macromolecules should have a collapsed coil configuration during injection into the reservoir to reduce both pumping costs and shear degradation at the well-head. Also, polymer coils should expand after injection to increase their solution extensional viscosity within the reservoir. The desired complex solution behavior may be achieved with synthetic polymers that can change their macromolecular conformation upon encountering certain environmental stimuli such as variations in solution temperature, pH, and electrolyte concentration.

In our last report, we discussed solution thermodynamic theory that described changes in polymer coil conformation as a function of solution temperature and polymer molecular weight. These polymers contained no ionic charges. In this report, we expand polymer solution theory to account for the electrostatic interactions present in solutions of charged polymers. Polymers with ionic charges are referred to as polyions or polyelectrolytes. Findings presented in this report will facilitate the design of new polyelectrolytes for improved sweep efficiency during polymer flooding. The scaling theory of polyelectrolyte solutions was found to be useful for determining the acceptable experimental conditions for obtaining valid solution intrinsic viscosities.

TASK 1: Polymer Synthesis

Background

Various zwitterionic polymers have been investigated in our laboratories due to their unique responsiveness to saline media.[1] Unlike polyelectrolytes (PEs), which bear *either* anionic or cationic charges, polyzwitterions (PZs) bear *both* anionic and cationic functionalities. PZs may be categorized as polyampholytes (anionic and cationic charges on *separate* repeat units) or polybetaines (anionic and cationic charges on the *same* repeat unit). In aqueous solution, PEs generally collapse with increasing ionic strength due to the screening of intramolecular repulsions between like charges along the polymer backbone.[2] This phenomenon, known as the polyelectrolyte effect, tends to impair the performance of PEs in applications where the polymers encounter saline media. In contrast to PEs, PZ solutions exhibit an antipolyelectrolyte effect in which the polymer adopts a more expanded conformation with increasing ionic strength.[3] This effect is attributed to the screening of intramolecular attractions between the pendant anionic and cationic moieties along the polymer backbone by the small molecule electrolytes. The increase in hydrodynamic size is also accompanied by an increase in solution viscosity, making PZs ideal candidates for salt-tolerant viscosifiers.

Another area of interest in our laboratories is the synthesis of hydrophobically modified (HM) water-soluble polymers via micellar copolymerization and their solution behavior in aqueous media. These hydrophilic copolymers contain small amounts (typically ≤ 1 mol%) of hydrophobic comonomers that enable viscosification through intermolecular hydrophobic associations.[4] Often referred to as associative thickeners (ATs), the HM copolymers exhibit greater thickening efficiency and more complex rheological properties compared to their unmodified counterparts. Several polymer systems investigated by our group have proven to be effective ATs with pH- and shear-responsive behavior.[5,6,7,8,9,10,11] Both the PZs and the ATs that have been the focus of our investigations demonstrate extremely high potential for application in areas such as enhanced oil recovery, drag reduction, coatings, personal care, and cosmetics.

Recently, efforts have been made to produce associative PZs that combine the benefits of PZ salt tolerance and HM copolymer thickening efficiency. Candau and coworkers have reported the micellar copolymerization of acrylamide, sodium 2-acrylamido-2-methylpropanesulfonate (NaAMPS), 3-(methacryloyloxyethyl)trimethylammonium chloride (MOETAC), and either *N*,*N*-dihexylacrylamide or *N*-ethylphenylacrylamide as the hydrophobic comonomer to yield HM polyampholytes.[12] The resulting HM polyampholytes exhibited both salt- and shear-responsive rheological behavior. Winnik and Wiyazawa have prepared phosphorylcholine-based HM polybetaines via post-polymerization modification of HM poly(*N*-isopropylacrylamide) with pendant amine moieties, and the solution behavior of the HM polybetaines was examined in mixed aqueous-organic media.[13,14] Due to high levels of phosphobetaine and hydrophobic comonomer incorporation and the random sequence of comonomer incorporation, the polymers tended to behave as polymeric micelles and were not examined as ATs.

It is well-known that the rheology of polymer solutions can be readily enhanced by the addition of surfactants as indicated in numerous literature studies.[11,15,16,17,18,19] Most research in this area has focused on the interaction of nonionic polymers with charged surfactants[20,21,22,23,24,25,26,27,28] and the interaction of PEs with surfactants of opposite charge.[29,30,31,32,33,34] PE-surfactant systems having the same charge have also been investigated.[11,15,16,19,35] In these studies, the polymers are usually hydrophobically modified to induce attraction between the polymer and the surfactant.

Relatively few studies of the interaction of surfactants with HM PZs have been conducted. Bekturov and coworkers studied the effect of adding SDS and cetyltrimethylammonium chloride (CTAC) to a polyampholytic system.[36] The addition of either surfactant to the polyampholyte solution produced a decrease in viscosity, although the effect of SDS was more pronounced than that of CTAC. Unlike PE-surfactant complexes, which tend to precipitate at certain ratios of PE to surfactant, the polyampholyte-surfactant complexes remained soluble over the entire composition range studied. The group postulated that the hydrophilic portions of the polyampholyte chain prevented precipitation of the polymer-surfactant complexes. More recently, Zana and coworkers have examined the interactions of polyampholyte terpolymers based on AM, NaAMPS, and MOETAC with either SDS or tetradecyltrimethylammonium bromide. The study revealed that polyampholyte-surfactant interactions were highly dependent on the charge balance of the polyampholytes and the charge of the surfactant employed.[37]

The goal of this current research is to examine the solution behavior of AM-based HM polybetaines containing either sulfobetaine or carboxybetaine comonomers in response to various external stimuli, including changes in solution pH, electrolyte concentration, and the addition of anionic, cationic, zwitterionic, and nonionic surfactants. For this study, terpolymers composed of acrylamide (AM), either 3-(2-acrylamido-2-methylpropanedimethylammonio)-1-propanesulfonate, (AMPDAPS) or (4-(2-acrylamido-2-methylpropyldimethylammonio) butanoate (AMPDAB), and *N*-butylphenylacrylamide (BPAM) (Figure 1) were synthesized using micellar copolymerization techniques to yield HM polybetaines. The HM polybetaines investigated in this work combine the unique attributes of both PZs and ATs. Additionally, the HM polycarboxybetaines are pH-responsive because of their carboxylic acid functionality, thus allowing the HM polycarboxybetaines to exhibit PE, PZ, or combined PE-PZ behavior. The solution behavior of the terpolymers was studied using surface tension and rheological techniques, and models are proposed to explain solution behavior as functions of pH, salt concentration, and surfactant addition.

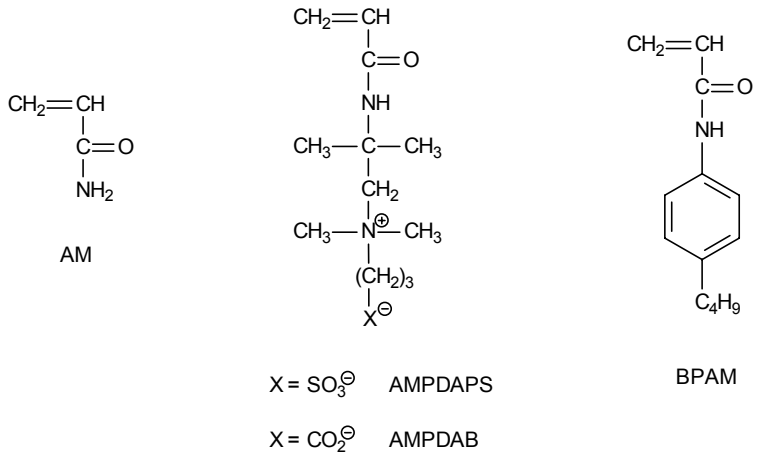

Figure 1. Monomers employed in synthesis of HM polybetaines via micellar copolymerization.

Experimental

Materials

AMPDAPS,[38] AMPDAB,[39] and BPAM[5] were prepared according to previously reported synthetic procedures. Triton X-100 was purchased from Bio-Rad Laboratories. All other chemicals were purchased from Aldrich and used as received except where indicated. Potassium persulfate (KPS) was recrystallized twice from water.

Terpolymer Synthesis

Terpolymers of AM, BPAM, and either AMPDAPS or AMPDAB were synthesized via micellar copolymerization in aqueous media using KPS as the initiator (Figure 2). The total monomer concentration was 0.44 M, and the ratio of total monomer concentration to initiator concentration was 3000. The feed ratio of BPAM was held constant at 0.5 mol %, and the SDS used to solubilize the BPAM was added at a SDS:BPAM ratio of 40:1. The amounts of AM and betaine comonomer in the feed were varied such that the percentages of betaine in the feed were 5 mol % (low charge density) or 25 mol % (high charge density), with the balance of the monomer feed being comprised of AM. A typical terpolymer polymerization procedure is described as follows:

To a 500 mL, three-neck round bottom flask equipped with mechanical stirrer and N_2 inlet/outlet was added DIH_2O (225 mL). The flask was immersed in a 50 °C constant temperature bath, and the contents were sparged with N_2 for one hour. SDS (5.71 g, 0.020 mol) was added to the flask and allowed to dissolve, followed by the addition of BPAM (101.0 mg, 0.50 mmol). Solubilization of BPAM was complete after 45 min, as indicated by the transparent appearance of the reactor contents. AM (5.24 g, 0.074 mol) and AMPDAPS (7.24 g, 0.025 mol) were then added to the flask and allowed to stir for 10 min. KPS (8.9 mg, 0.033 mmol) dissolved in 5 mL of degassed DIH_2O was then added to the flask via syringe. The polymerization was allowed to proceed under a N_2 atmosphere for 4.5 h. Stirring speed was

adjusted to maintain a shallow vortex in the reaction medium. Polymerization was terminated by precipitating the polymer in an excess of acetone. The precipitated polymer was redissolved in DIH_2O, purified by dialysis against DIH_2O using Spectra-Por No. 4 dialysis tubing (molecular weight cut-off = 12-14,000 g/mol) for two weeks, and isolated via lyophilization.

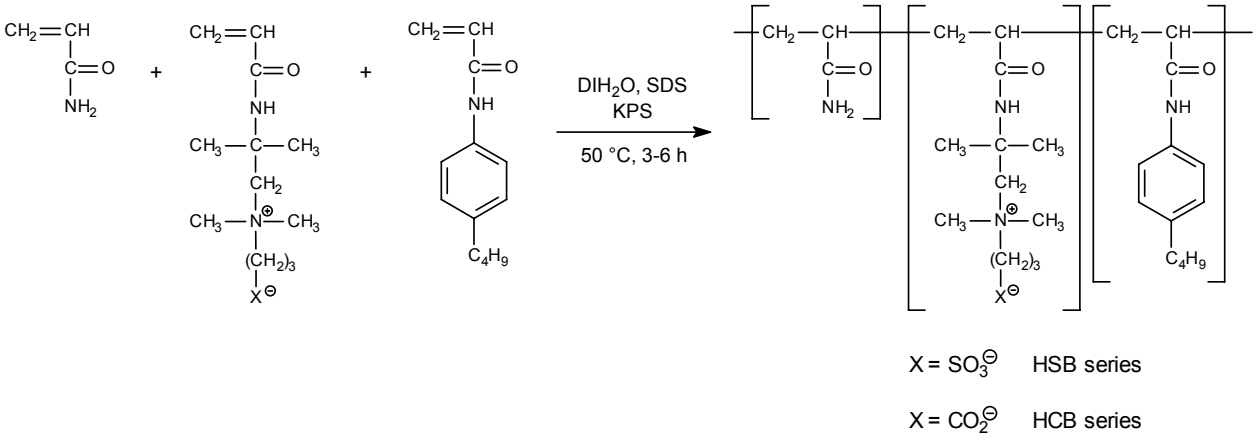

Figure 2. Synthesis of HM polybetaine terpolymers.

The HM polybetaine terpolymers are designated as either HSB# (sulfobetaine series) or HCB# (carboxybetaine series), where # indicates the mol % of betaine comonomer present in the feed. Copolymers lacking either BPAM or betaine comonomer were prepared for the purpose of performing comparative studies. For example, copolymers of AM and AMPDAPS or AMPDAB were synthesized using the same procedure outlined above, but in the absence of BPAM. These copolymers are designated SB# and CB#, respectively. A nonionic copolymer of AM and BPAM was prepared via micellar copolymerization using the above procedure and is designated HAM. A polyacrylamide homopolymer was also synthesized under the micellar conditions and is designated PAM. The sample nomenclature and target compositions of the HM polybetaines and control polymers synthesized for this study are indicated in Table 1.

Instrumentation and Analysis

UV-VIS Spectroscopy: UV spectra were obtained using a Hewlett-Packard Model 8452A Photodiode-Array Spectrophotometer. The fixed resolution was 2 nm. The sample optical density was maintained below 1.0 and the model compound used was *N*-(4-butyl)phenylamidopropionic acid.[5]

Table 1. Target compositions of HM polybetaines and control polymers.

Sample ID	AM[a] (mol %)	AMPDAPS[a] (mol%)	AMPDAB[a] (mol%)	BPAM[a] (mol %)
HSB5	94.5	5	—	0.5
HSB25	74.5	25	—	0.5
SB5	95.0	5	—	—
HCB5	94.5	—	5	0.5
HCB25	74.5	—	25	0.5
CB5	95.0	—	5	—
HAM	99.5	—	—	0.5
PAM	100.0	—	—	—

[a] Indicates mol% monomer present in feed ratio

^{13}C NMR and ^{1}H NMR Spectroscopy: ^{13}C NMR and ^{1}H NMR spectra were obtained with a Bruker AC 200 spectrometer and processed using software provided by the manufacturer. Betaine comonomer incorporation was determined via inverse gated decoupled ^{13}C NMR with a delay time of 6 s.

Compositional Analysis: Terpolymer compositions were determined using results from inverse gated decoupled ^{13}C NMR and UV/VIS experiments. The representative relationships used to calculate the mol % of each monomer in the terpolymers are as follows:

$$x = (C - z) - y \tag{1}$$

$$Y = \frac{\dfrac{y}{MW_y}}{\left(\dfrac{(C-z)-y}{MW_x}\right) + \left(\dfrac{y}{MW_y}\right) + \left(\dfrac{z}{MW_z}\right)} \tag{2}$$

where C = total polymer concentration in UV-Vis sample solution in g/dL, x = AM concentration in g/dL, y = betaine monomer concentration in g/dL, Y = betaine comonomer incorporation in mol % (from ^{13}C NMR), z = BPAM concentration in g/dL (from UV/Vis), and MW_x, MW_y, and MW_z, are the molecular weights of AM, the betaine comonomer (AMPDAPS or AMPDAB), and BPAM, respectively.

Classical Light Scattering: Classical light scattering (LS) measurements were performed on a Brookhaven Instruments BI-200SM automatic goniometer equipped with a Spectra-Physics 127 laser (632.8 nm) and BI-2000 autocorrelator. Berry plots were obtained using software provided by the manufacturer. Data points for classical LS analysis were taken at 60 °, 70 °, 90 °, 100 °, 110 °, and 135 ° and at 25 °C. The polymers were examined in 0.5 M NaCl and purified via

extensive centrifugation in an Eppendorf 5415C ultracentrifuge. Errors in reported molecular weights ranged from 0.4 to 5.8 %. Refractive index increments were measured using a Chromatix KMX-16 laser differential refractometer operating at 632.8 nm and 25 °C.

Potentiometric Titration: Potentiometric titrations were conducted using an Orion model 900A Titration System under an inert atmosphere. Titration samples were purged with N_2 until a constant pH was maintained. The experimental error associated with the titration was ±0.05 pH units.

Solution Rheology: Solution viscosity measurements were performed using a Contraves LS-30 low shear rheometer. The measurements were conducted at 25 °C and at a shear rate of 5.96 s^{-1}. Reported viscosities are the average of five measurements. The upper viscosity limit of the rheometer was taken as 125 cP.

Surface Tensiometry: A Kruss K12 Processor Tensiometer was utilized to conduct Wilhemy plate surface tension measurements. Doubly distilled water (surface water) was used to prepare all surface tension solutions. A minimum surface tension reading of 72 mN/m confirmed a lack of surface contaminants in the water. Surfactants were purified as follows: SDS was recrystallized three times from ethanol, DTAB was recrystallized three times from an ethyl acetate/ethanol (10/1 v/v) solution, and SB3-12 was recrystallized twice from 2-propanol. Polymer solutions were prepared at a concentration of 0.2 g/dL. An aliquot of polymer solution was used to prepare polymer-surfactant solutions to assure consistency of polymer concentration during the experiment. The necessary amount of surfactant was added to the polymer solution to bring the surfactant concentration to the desired value. Experimental error in reported surface tension values is ≤ ±1.5 %.

Results and Discussion

Polymer Synthesis

AM-based HM polybetaine terpolymers were synthesized via micellar copolymerization using the feed ratios outlined in Table 1. The terpolymers contained either sulfobetaine (AMPDAPS) or carboxybetaine (AMPDAB) comonomers at low (5 mol %) and high (25 mol %) charge densities, and the single-tailed alkylaryl acrylamide monomer BPAM was employed as the hydrophobic comonomer. The HM polysulfobetaine and HM polycarboxybetaine terpolymers have been designated as the HSB# and HCB# series, respectively, where # indicates the targeted level of betaine comonomer incorporation. To enable comparative studies that would distinguish between the effects of betaine and hydrophobic comonomer incorporation, it was necessary to synthesize the control (co)polymers CB5, SB5, HAM, and PAM (refer to Table 1 for target compositions).

The average number of BPAM monomers per micelle was calculated to be N_H = 1.65 using Equation 3, where [BPAM] is the concentration of BPAM in mol/L, N_{agg} is the aggregation number of SDS ($N_{agg} \approx 62$ for SDS), [SDS] is the concentration of SDS in mol/L, and cmc_{SDS} is

the critical micelle concentration of SDS in mol/L (8.1×10^{-3} mol/L).[7] It was assumed that the presence of the betaine comonomers in the micellar polymerization medium did not change the aggregation number of SDS significantly during HM terpolymer synthesis. This is a reasonable assumption, as the betaine monomers are entirely hydrophilic and lack amphiphilic character that would cause them to comicellize with SDS.

$$N_{\mathrm{H}} = \frac{[\mathrm{BPAM}] \times N_{\mathrm{agg}}}{[\mathrm{SDS}] - cmc_{\mathrm{SDS}}} \tag{3}$$

Polymer Characterization

Compositional Analysis: Polymer compositions (Table 2) were determined from the combined results of UV and inverse gated decoupled ^{13}C NMR spectroscopic analysis. The carbonyl region of a typical ^{13}C NMR spectrum used to determine betaine comonomer incorporation is shown in Figure 3 (note that the carbonyl peak for BPAM is undetectable due to low incorporation). The values for betaine comonomer incorporation agree reasonably well with the target values (Table 1), given the margin of error (typically ≥ 5%) associated with ^{13}C NMR as a quantitative analytical tool. Although polymerizations were halted at < 50% conversion to avoid compositional drift, BPAM incorporation in the HM samples is consistently higher than the target value of 0.5 mol %. These results are consistent with those reported by Middleton and coworkers[5] for BPAM-modified AM copolymers that were synthesized under similar micellar conditions. Additionally, Candau and coworkers have reported copolymer drift and higher molar incorporations of hydrophobes with single tails.[40]

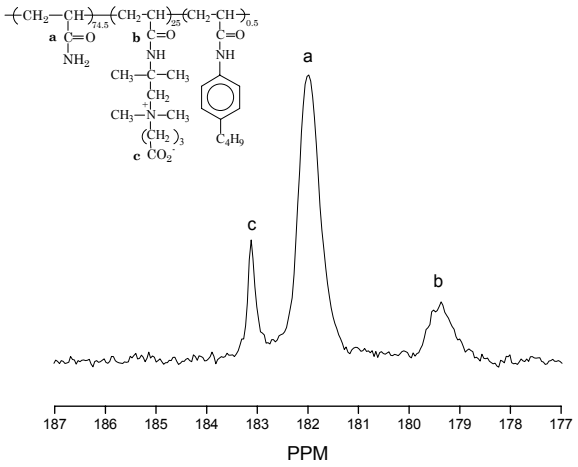

Figure 3. Carbonyl region of HCB25 ^{13}C NMR spectrum.

Table 2. Compositional data for the HM polybetaine terpolymers and the control samples.

Sample ID	AM (mol %)	Betaine comonomer[a] (mol %)	BPAM[d] (mol %)
HSB5	95	4.1[b]	0.88
HSB25	76	23[b]	1.00
SB5	95	5.0[b]	—
HCB5	96	3.6[c]	0.64
HCB25	82	17[c]	1.00
CB5	91	8.9[c]	—
HAM	99.5	—	0.55

[a] Determined via inverse gated decoupled ^{13}C NMR

[b] AMPDAPS

[c] AMPDAB

[d] Determined via UV-Vis spectroscopy

Light Scattering Analysis: Classical light scattering data for the polymers synthesized in this study are given in Table 3. Values of weight-average molecular weight (M_w) range from 4.19×10^5 g/mol (HCB25) to 1.29×10^6 g/mol (HCB5). All hydrophobically modified polymers except HSB5 exhibit negative second virial coefficients (A_2), a commonly observed phenomenon for associative polymers analyzed via classical light scattering in aqueous media.

Table 3. Classical light scattering data for the HM polybetaines and the control samples.

Sample ID	M_w[a] (10^6 g/mol)	A_2[a] (cm^3 mol/g^2)
HSB5	0.827	1.3×10^{-3}
HSB25	1.13	-4.82×10^{-5}
SB5	0.819	4.08×10^{-4}
HCB5	1.29	-9.18×10^{-5}
HCB25	0.419	-5.77×10^{-3}
CB5	1.16	1.36×10^{-4}
HAM	0.806	-2.52×10^{-3}
PAM	0.850	4.2×10^{-3}

[a] Determined in 0.5 M NaCl at 25 °C

Potentiometric Titration: Potentiometric titrations were performed on the carboxybetaine polymers (Figure 4). The pK_a values were found to increase with increasing BPAM incorporation. The pK_a of CB5 is 4.1, which is typical of carboxybetaines, however, the pK_a

values of HCB5 and HCB25 are 6.2 and 7.2, respectively. It is postulated that increasing hydrophobe incorporation increases pK_a values due to shifts in Henderson-Hasselbach equilibrium as a consequence of restricted polymer conformation and local dielectric effects. These results indicate that both HCB5 and HCB25 possess some polyelectrolyte character at ambient pH.

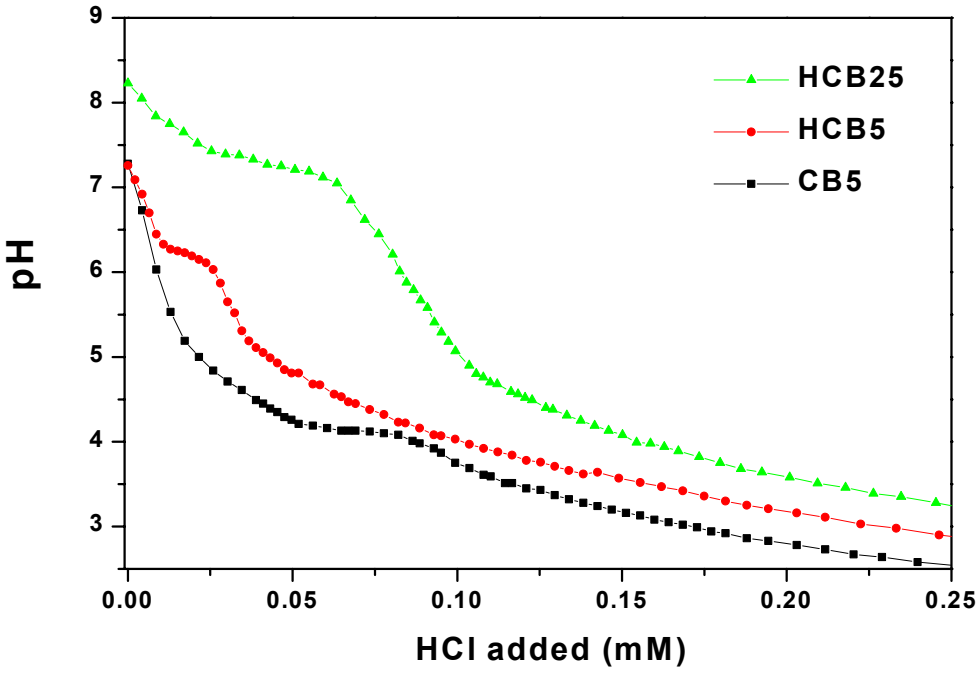

Figure 4. Potentiometric titration curves for the HM carboxybetaine terpolymers (HCB25 and HCB5) and the carboxybetaine copolymer (CB5).

Polymer Solution Rheological Behavior

Overall, the polymer solutions demonstrated behavior characteristic of HM- and/or PZ-type polymers, with the exception of HCB25, which showed unusual, yet remarkable, behavior in several rheological experiments. The high level of AMPDAB incorporation in HCB25 is presumed to be responsible for the anomalous behavior of HCB25. Results from each rheological experiment are given in the following section along with possible explanations for the observed behavior based on the structure and composition of the polymers examined.

An important factor to consider when examining polymer solution behavior is the critical overlap concentration (c^*) of the polymer solution. Below c^* (i.e. in the dilute regime), individual polymer chains are essentially isolated from each other, and the solution viscosity is dependent on the individual contributions of the solvated polymer coils. At c^*, polymers in solution start to become entangled, and the solution viscosity begins to increase more rapidly with increasing polymer concentration. Above c^* (i.e. in the semi-dilute regime), the solution viscosity is now dependent on the individual contributions of the polymer coils plus the entanglements between the network of overlapping coils. For solutions of associative (e.g. hydrophobically or electrostatically associating) polymers, network formation occurs at lower concentrations than for nonassociative polymers due to intermolecular associations that occur

prior to chain entanglement.[4142] This network formation is accompanied by a dramatic increase in solution viscosity. For this reason, associative polymers are typically more efficient thickeners than their unmodified counterparts because the intermolecular network formation offers an additional viscosification mechanism above *c**.

Viscosity profiles of the HM sulfobetaine terpolymers and relevant control (co)polymers are shown in Figure 5. HSB5 exhibits the greatest increase in viscosity with increasing polymer concentration, followed by HAM, SB5, HSB25, and PAM. Based on this data, several comparisons and explanations may be offered. Peiffer and Lundberg have reported that AM-based polyampholytes containing charge densities of less than 10 mol % mainly associate intermolecularly at concentrations of 1 to 3 g/dL, whereas polyampholytes with charge densities greater than 10 mol % associate intramolecularly.[43] Their zwitterionic systems incorporated quaternary amines and sulfonate groups similar to those employed in the AMPDAPS-containing samples. Upon close inspection of the viscosity data, the trend in Figure 5 appears to be consistent with the results reported by Peiffer and Lundberg. The polymer with low zwitterionic monomer incorporation, HSB5, attains higher viscosity values than the analogous polymer with higher zwitterionic incorporation, HSB25, despite its lower molecular weight and comparable hydrophobe incorporation. It is known that interaction between sulfobetaine units is relatively strong and is thought to be the reason some acrylamide based polymers containing large amounts (≥ 60 mol %) of sulfobetaine comonomer are insoluble in DIH_2O.[38] It is postulated that at 25 mol % sulfobetaine incorporation, zwitterions on the same chain are present in sufficient concentrations to severely restrict polymer conformation yet still from soluble intramolecularly-associated complexes.

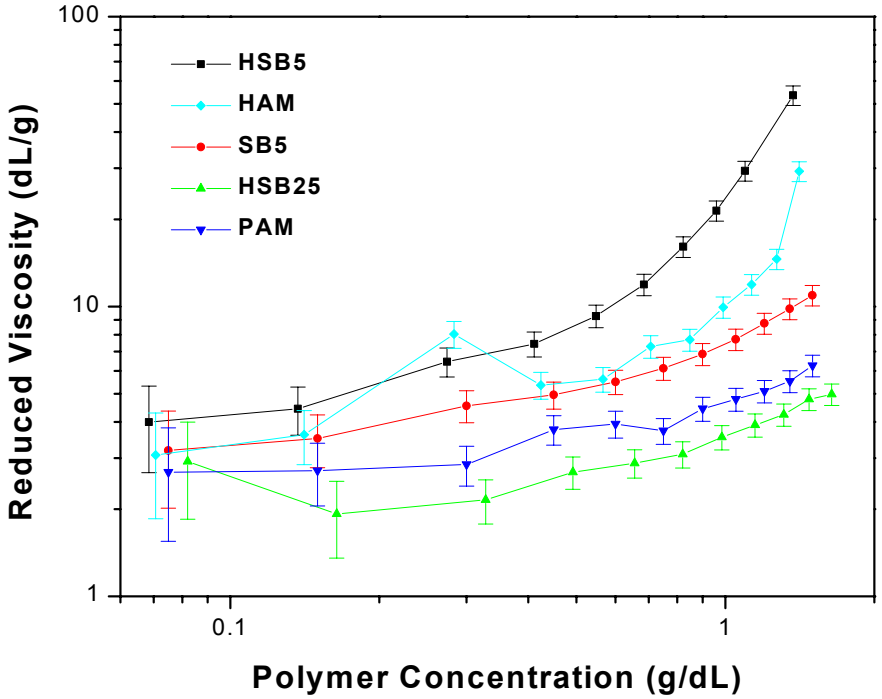

Figure 5. Viscosity profiles of HM sulfobetaine terpolymers and control polymers in DIH_2O at ambient pH (7.5 ± 0.5).

A meaningful comparison may be made between SB5 and HAM due to similar molecular weight values. In the concentration range studied, HAM shows sharp a upturn in reduced viscosity as a function of polymer concentration, while SB5 does not; this provides evidence that HAM passes through *c** in this concentration range and that there are intermolecular associations of the BPAM moieties on the HAM chains. It is also reasonable to conclude that the hydrophobic association of BPAM moieties has a greater effect on the solution rheology of HSB5 than does the electrostatic association of AMPDAPS moieties.

The rheological behavior of the HM carboxybetaine terpolymers and relevant control (co)polymers was also studied as a function of concentration at ambient pH (Figure 6). After HCB25 (discussed later), HCB5 appears to be the most efficient thickener due to hydrophobic modification. Incorporation of carboxybetaine moieties appears to have a substantial effect on viscosity enhancement, presumably due to the greater hydrophilicity of the carboxybetaine relative to that of the sulfobetaine.[44,45] CB5 is a more effective viscosifier than HAM, in contrast to case of SB5 and HAM mentioned earlier. The molecular weight of CB5 is 1.16×10^6 g/mol, while that of HAM is 8.06×10^5 g/mol. Although molecular weight differences may be partly responsible for this behavior, the increased hydrophilicity of CB5 most likely plays a more crucial role, allowing CB5 to adopt a more expanded conformation than HAM. HCB25 exhibits a much higher solution viscosity than the other carboxybetaine-containing polymers in DIH_2O, despite its relatively low molecular weight. Due to the high viscosity of the HCB25 solutions in DIH_2O, measurements were made at lower polymer concentrations than the other samples to prevent the upper viscosity limit of the LS-30 rheometer from being exceeded.

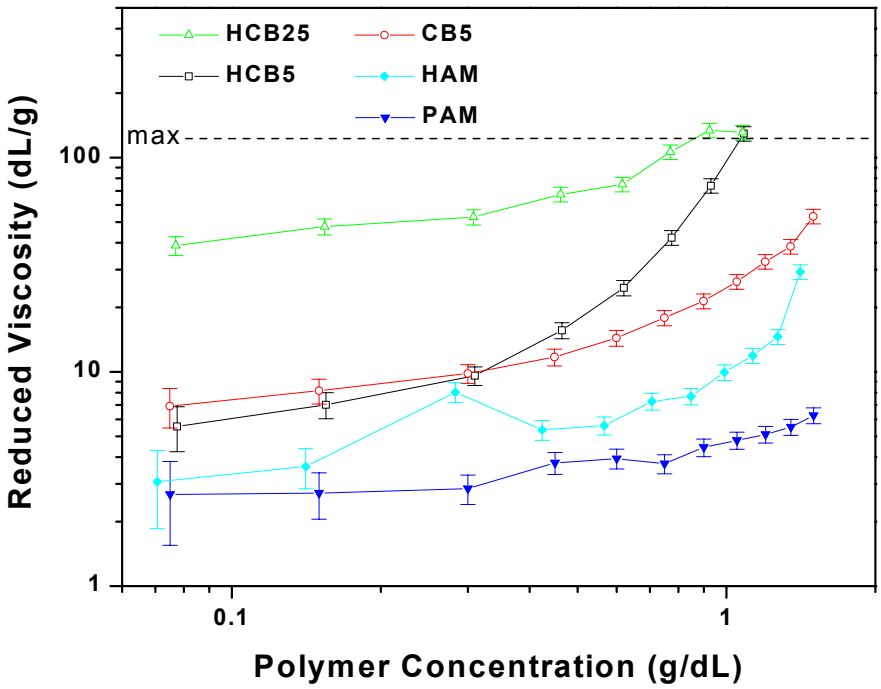

Figure 6. Viscosity profiles of HM carboxybetaine terpolymers and control polymers in DIH_2O at ambient pH (7.5 ± 0.5).

Effect of Salt: The effect of NaCl addition on the solution viscosity of the HM sulfobetaine terpolymers and relevant control (co)polymers was investigated (Figure 7). HSB25, HSB5, and SB5 were found to respond to the addition of salt at a polymer concentration of 0.4 g/dL. The increase in viscosity at higher salt concentrations is consistent with the disruption of intramolecular zwitterionic associations due to shielding by the added ions. HAM demonstrates a viscosity decrease at low NaCl concentration as a consequence of increased intramolecular hydrophobic association in the presence of salt. Figure 8 depicts the effect of NaCl concentration on the viscosity behavior of the HM carboxybetaine terpolymers and relevant control (co)polymers. A very slight initial decrease in viscosity is seen for HCB5, followed by an increase. The initial decrease may be due to a slight polyelectrolyte effect, followed by typical polyampholyte response to electrolytes. The small polyelectrolyte effect is likely due to the relatively high pK_a (6.2) of this polymer (Figure 4). HCB25 demonstrates classical polyelectrolyte in the presence of very low concentrations (e.g. 1 mM) of NaCl; the solution viscosity of HCB25 drops dramatically and does not increase on further salt addition (i.e. the antipolyelectrolyte effect is not observed).

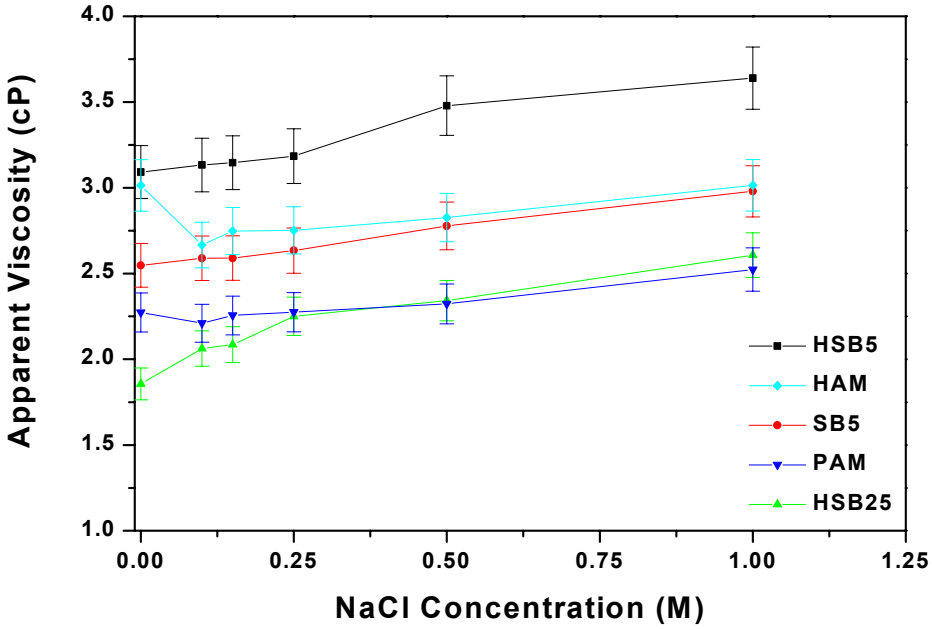

Figure 7. Reduced viscosity as a function of NaCl concentration for the HM sulfobetaine terpolymers and control polymers. Polymer concentration = 0.4 g/dL, ambient pH (7.5 ± 0.5).

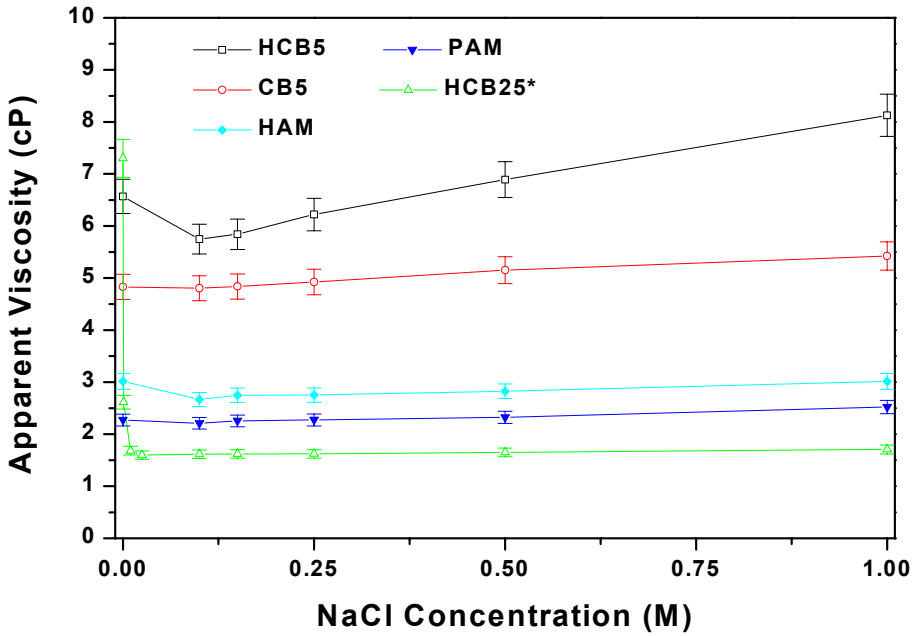

Figure 8. Apparent viscosity as a function of NaCl concentration for the HM carboxybetaine terpolymers and control polymers. Polymer concentration = 0.4 g/dL, except for HCB25, where polymer concentration = 0.1 g/dL, ambient pH (7.5 ± 0.5).

Effect of pH: The ambient pH of most polymer solutions in this study ranged from 7.0 - 7.5. Adjustment of pH was readily achieved via the addition of small aliquots of concentrated HCl or NaOH. Not surprisingly, no effect of pH on solution viscosity was detected for sulfobetaine-containing polymers. This is expected due to the very low reported pK_a (≈ –9) of the sulfonate moiety.[45] As seen in Figure 9, a maximum in viscosity at pH ≈ 3 is apparent in all carboxybetaine polymers displayed. This phenomenon has been previously reported and is due to polycation formation as pH is lowered, thus causing an increase in viscosity due to intramolecular charge-charge repulsion.[39] At pH values below 3, intramolecular association of the carboxylic acid groups and the excess ionic strength of the solutions become significant, inducing collapse of the polyelectrolyte coils and the corresponding decrease in viscosity.[8,46]

HCB25 solutions exhibit unusual pH-responsive behavior. When HCB25 is dissolved in DIH_2O, the solution pH is typically observed to be around pH 7.5. At pH 3, all three carboxybetaine-containing polymers exhibit a maximum in viscosity due to the polycation nature of the polymers when the carboxylate groups of the betaine are protonated. However, unlike HCB5 and CB5, HCB25 exhibits a local maximum in viscosity at pH 7.5 – 8.0, followed by a sharp decline in solution viscosity at successively higher pHs (Figure 9). An additional viscosity study as a function of pH was performed on HCB25 at a lower polymer concentration (Figure 10) to determine if the anomalous pH response of HCB25 was being cause by a pH-induced transition from dilute to semidilute conditions (i.e. pH-induced chain overlap). Unexpectedly, the relative size of the anomalous pH 7.5 peak increased, while the pH 3 peak maximum decreased.

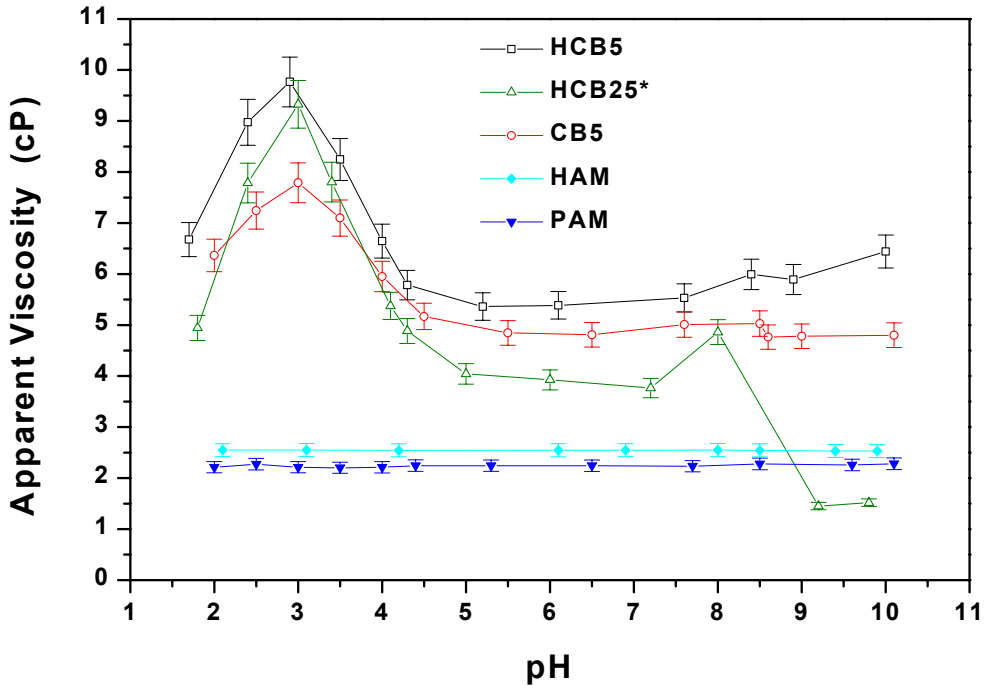

Figure 9. Apparent viscosity as a function of pH for the HM carboxybetaine terpolymers and control polymers. Polymer concentration = 0.4 g/dL, except for HCB25, polymer concentration = 0.1 g/dL.

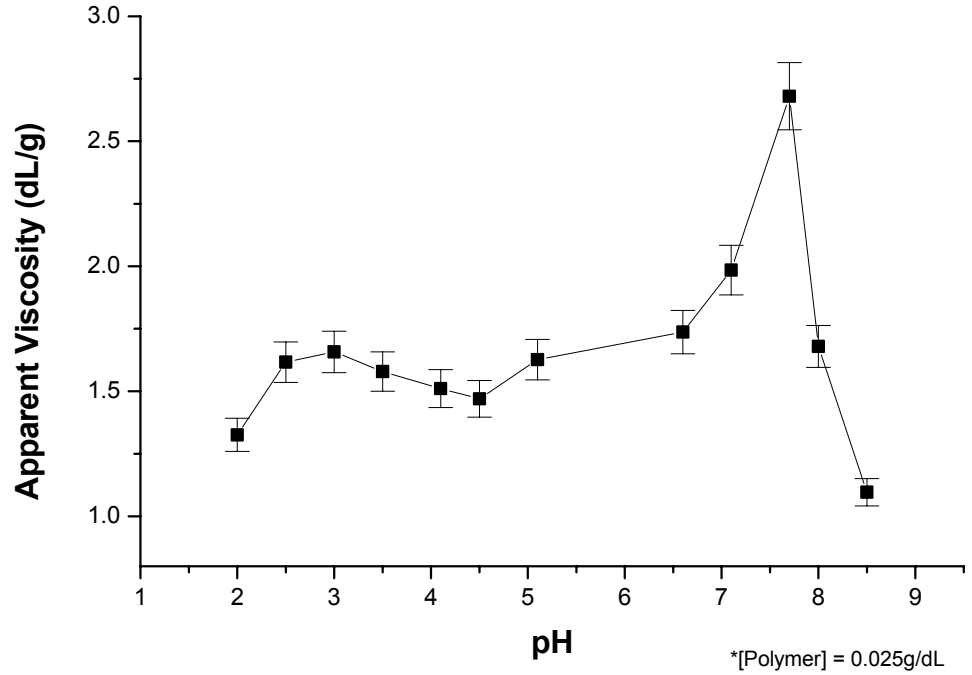

Figure 10. Apparent viscosity of HCB25 as a function of pH in DIH_2O. Polymer concentration = 0.025 g/dL.

Based on experimental observations, the anomalous behavior of HCB25 can be rationalized by the following conceptual model which describes the associative nature of the polymer as a function of pH. Recall that the pK_a of HCB25 (pK_a = 7.2) is higher than that of typical carboxybetaines (pK_a = 4), thus the majority of carboxybetaine units on this polymer will be protonated in the low to intermediate pH range (i.e. pH 2 through pH 7.5, the ambient solution pH of HCB25 in DIH_2O). In this pH range, HCB25 behaves as a cationic polyelectrolyte, and intra- and intermolecular electrostatic associations between carboxybetaine units are not possible, as those repeat units are not in their zwitterionic form. While zwitterionic associations are not possible, the carboxylic acids of the protonated betaine are capable of hydrogen-bonding associations with other betaine moieties, as well as with the pendant amide groups of the PAM backbone. (This phenomenon has been observed in HM copolymers of AM with acrylic acid.[8]) In addition to hydrogen bonding associations, the hydrophobic BPAM units are also capable of intra- and intermolecular association. At pH ≥ 8.0, the carboxybetaine moieties become fully ionized, and electrostatic associations between the zwitterionic species are possible. Simultaneously, the ability of the carboxylate groups form hydrogen bonds is eliminated at pH ≥ 8.0. The ability of the BPAM units to associate is assumed to remain unchanged above pH 8.0.

With the pH-dependence of the HCB25 association mechanisms in mind, the pH-responsive solution viscosity may now be considered in terms of polymer solution concentration. At low concentrations (e.g. 0.025 g/dL, Figure 10), HCB25 exhibits decreased solution viscosity from pH 2 through pH 7, where intramolecular hydrophobic associations coupled with intramolecular hydrogen bonding result in compact hydrodynamic volume of the polymer chains. As the solution pH is increased to pH 7.5, the intramolecular hydrogen bonding is diminished, leading to increases in hydrodynamic volume and the local maximum in solution viscosity. Above pH 7.5, the ionized carboxybetaine moieties undergo intramolecular associations that lead to chain collapse that further promoted by the intramolecular association of the hydrophobic BPAM moieties.

At higher solution concentrations (e.g. 0.1 g/dL, Figure 9), the maxima in HCB25 solution viscosity profiles are increased because the polymers approach the semidilute regime and can undergo intermolecular associations with appropriate stimuli. For example, at pH 3 the extended polycationic chains are capable of undergoing intermolecular hydrophobic and hydrogen bonding, hence the maximum in solution viscosity. Thus, the solution behavior of HCB25 is the result of a complex combination of electrostatic, hydrogen-bonding, and hydrophobic effects that are readily influenced by changes in polymer concentration, solution pH, and salt concentration.

Polymer-Surfactant Solution Behavior

Addition of surfactants (at concentrations below the surfactant *cmc*) to HM polymer solutions can increase the viscosity of polymer solutions, provided the complexes work in a cooperative manner to promote bridging between polymer chains.[15,17,19,47,48,49,50] The accepted model concerning associative complexes of HM polymers and surfactants involves formation of mixed micelles, or hemi-micelles, composed of polymer-bound hydrophobes comicellized with surfactant molecules (Figure 11, Pathway 1). If multiple polymer-bound hydrophobes from

different polymer chains participate in the same mixed micelle, a physical crosslink is formed between the polymer chains.[15,51] A dramatic increase in solution viscosity is often observed as these intermolecular physical crosslinks are formed. As the concentration of surfactant in the polymer solution is increased (approaching the *cmc*), the stoichiometry of the system will eventually be such that only one polymer-bound hydrophobe reamins per mixed micelle. At this point the physical crosslinks no longer exist, and the polymer-bound hydrophobes are sheathed in surfactant micelles adsorbed to the polymer chain. Surfactant-induced viscosity enhancement no longer occurs as this point due to the loss of the physical crosslinks. In HM polymer solutions above *c**, the soluiton viscosity in the presence of high concentrations of surfactant (i.e. surfactant concentration > *cmc*) is often lower than the original solution viscosity in the absence of surfactant.[52]

The electrostatic repulsions of charged hemi-micelles adsorbed along the polymer may cause chain expansion leading to an increase in viscosity below *c**.[53] In some cases the addition of surfactant to HM polymer solutions below *c** has been reported to cause viscosity reduction.[48,49,54,55] In this case, contraction of the polymer chain results from intramolecular interactions induced by hemi-micelles (Figure 11, Pathway 2).

Our goal in this research is to induce intermolecular associations, and thus enhanced viscosity, through the addition of surfactants to polymer solutions. Therefore, we selected polymer concentrations immediately preceding the onset of *c** to produce the viscosity enhancement through surfactant addition. (Based on the findings from the viscosity vs. polymer concentration experiments, we elected to conduct polymer-surfactant solution rheological studies at polymer concentrations of 0.4 g/dL.) The effects of surfactant addition on solution viscosity are readily probed on the macroscopic level via rheological analysis.

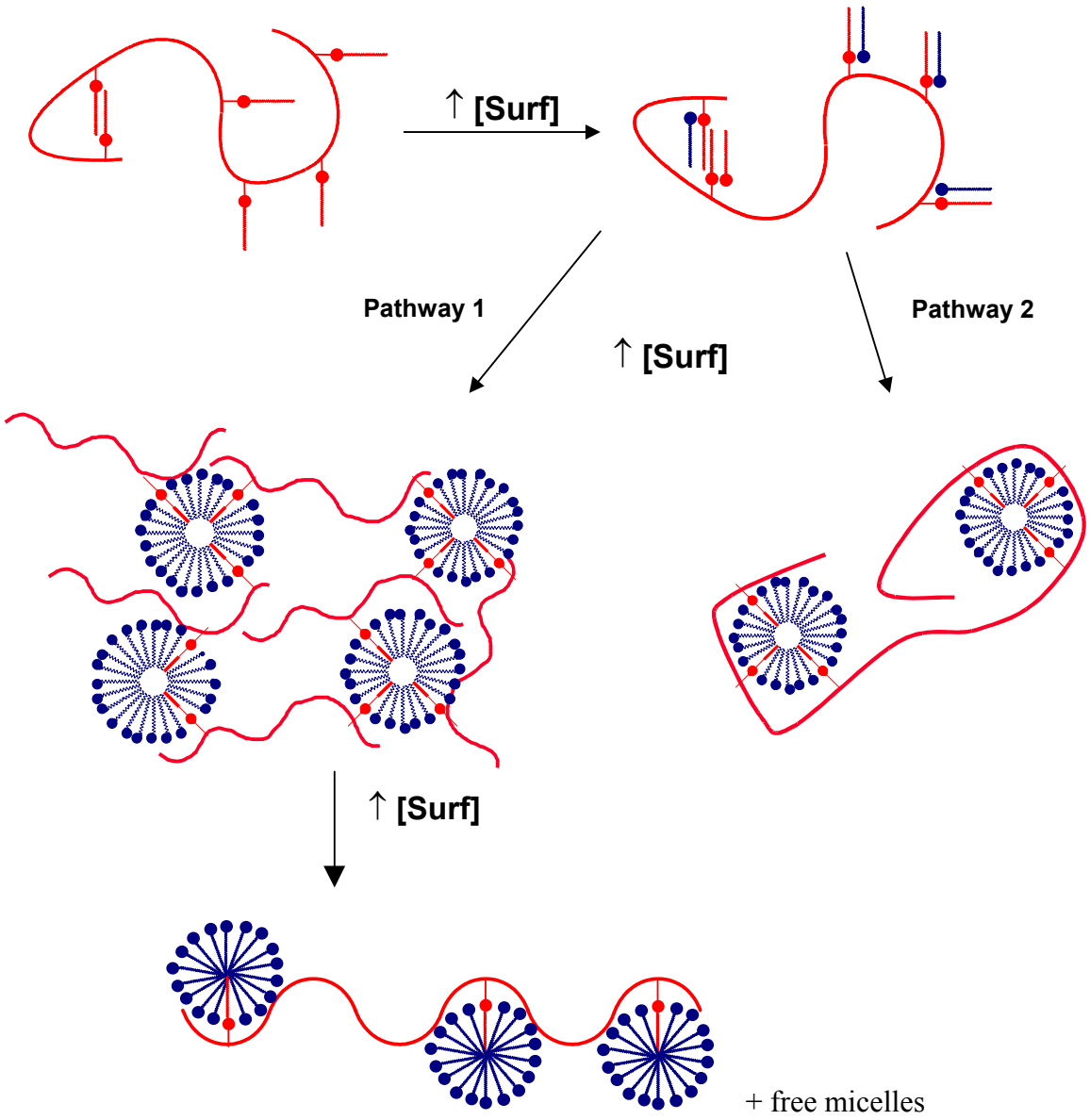

Figure 11. Proposed mechanisms of surfactant-induced viscosity enhancement in HM polymer solutions.

Surface tension experiments were also conducted to further probe the effects of surfactant addition to polymer solutions. Figure 12 depicts an idealized surface tension profile for a small molecule surfactant in aqueous solution.[53,56] As surfactant is added to water, a very small number of individual molecules dissolve in the bulk solution, thus having little effect on surface tension. This is the plateau region shown at very low concentrations. For some surfactants, this region is so small it is usually undetectable. As more surfactant is added, the molecules migrate to the air-water interface to minimize contact of their hydrophobic tails with water. The surface tension at the air-water interface is lowered as the concentration of surfactant at the interface increases. At the *cmc*, the chemical potential of surfactant adsorbed at the air-water interface becomes equal to the chemical potential for micelle formation. Thus, surfactant added in excess

of the *cmc* is preferentially solubilized in micelles, and the surface tension reaches a plateau value.

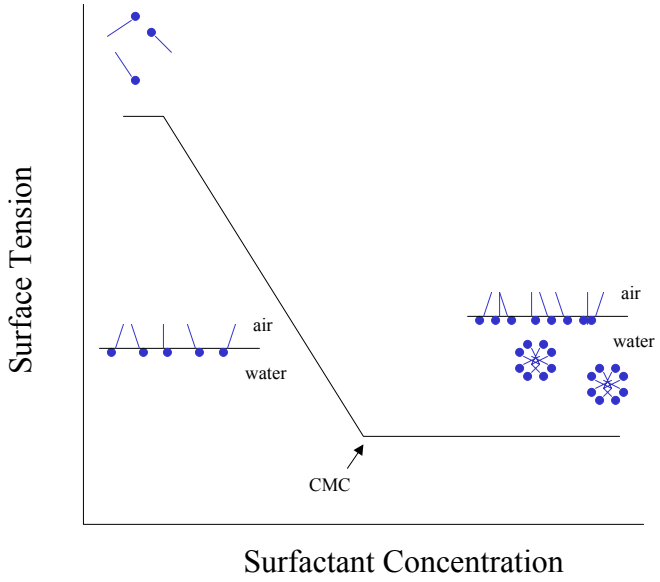

Figure 12. Idealized surface tension curve for small molecule surfactants.

The addition of a HM polymer to a surfactant solution modifies the surface tension profile.[53,56] An idealized model of this situation is shown in Figure 13. As before, an initial plateau region may or may not be detected (for simplicity, this region is omitted in Figure 13). As surfactant is added to the polymer solution, it first migrates to the air-water interface, lowering the surface tension. At the crossover concentration (C_1), the chemical potential becomes for favorable for polymer-surfactant interaction; the surface excess concentration of the surfactant remains unchanged at C_1 as surfactant interacts preferentially with polymer in the bulk solution. Upon reaching a saturation point (C_2), the chemical potential of surfactant migration to the air-water interface becomes favored, and the surface tension is lowered until the chemical potential of the surface becomes equal to that in a micelle. At C_2, any excess surfactant added to the polymer-surfactant solution will form micelles in solution. The point C_2 is detected as a plateau in the surface tension profile that has the same magnitude of the surface tension at the *cmc* in the absence of polymer.

Indeed, in experimentally observed systems, polymer-surfactant solution surface tension profiles deviate from ideality due to the dynamics of polymer conformation and polymer-surfactant interactions. Values of C_1 and C_2 are usually still detectable, but the surface tension plot between these points is typically curved due to changes in polymer-surfactant interaction, which may lead to changes in polymer conformation.

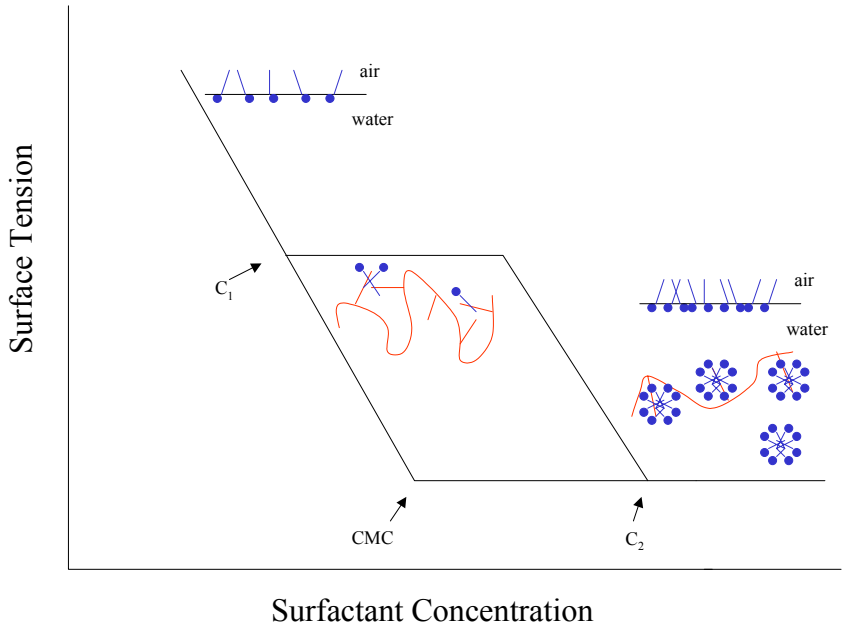

Figure 13. Idealized surface tension profile of a small molecule surfactant in the presence of polymer.[53,56]

Effect of Nonionic Surfactant: The effects of nonionic surfactants on the solution rheology of the HM polybetaine terpolymers and control (co)polymers were examined using Triton X-100, an ethoxylated nonylphenol-type surfactant. Figure 14 shows the effects of Triton X-100 addition to solutions of the HM polysulfobetaine terpolymers and the corresponding control (co)polymers. Of the polymers investigated, only HSB5 shows an increase in viscosity upon the addition of surfactant. The viscosity trend for this polymer is consistent with the polymer-surfactant interaction model depicted in Figure 11, Pathway 1, although the viscosity increase is small. HCB5 (Figure 15) displays a greater enhancement in viscosity due to the addition of Triton X-100 compared to the corresponding sulfobetaine polymer HSB5 (Figure 14). This viscosity increase is exemplary of comicellization of polymer and surfactant as shown in Figure 11, Pathway 1. The high charge density HM polybetaines HCB25 and HSB25 lacked any significant viscosity enhancement in all surfactant systems studied. In fact, HCB25 actually demonstrated a decrease in viscosity upon the addition of Triton X-100, indicating behavior similar to that depicted in Figure 11, Pathway 2.

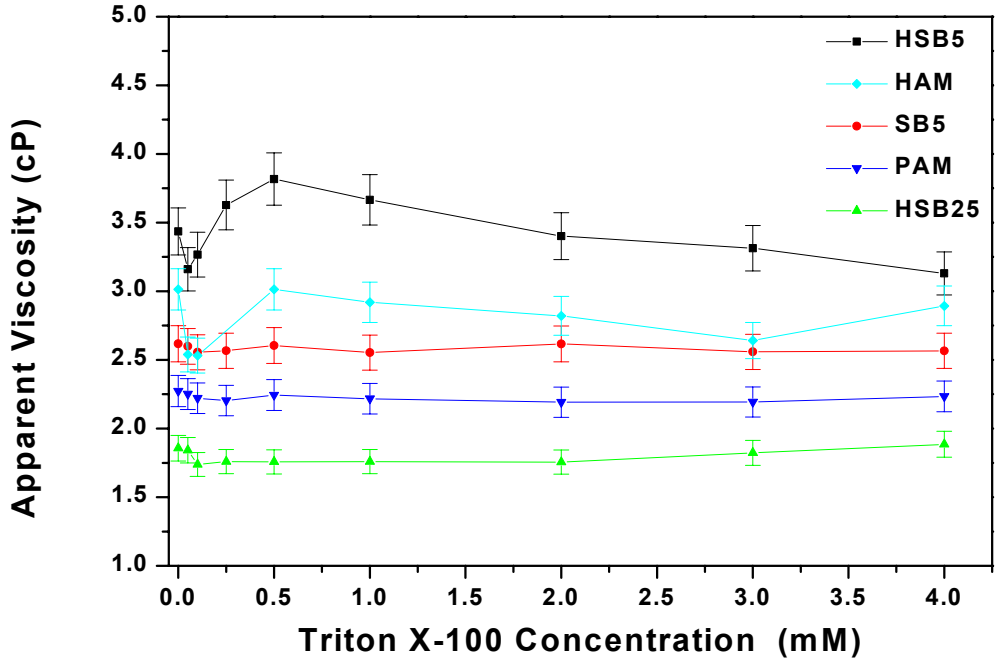

Figure 14. Apparent viscosity of the HM sulfobetaine terpolymers and the control polymers as a function of Triton X-100 concentration. Polymer concentration = 0.4 g/dL, ambient pH (7.5 ± 0.5).

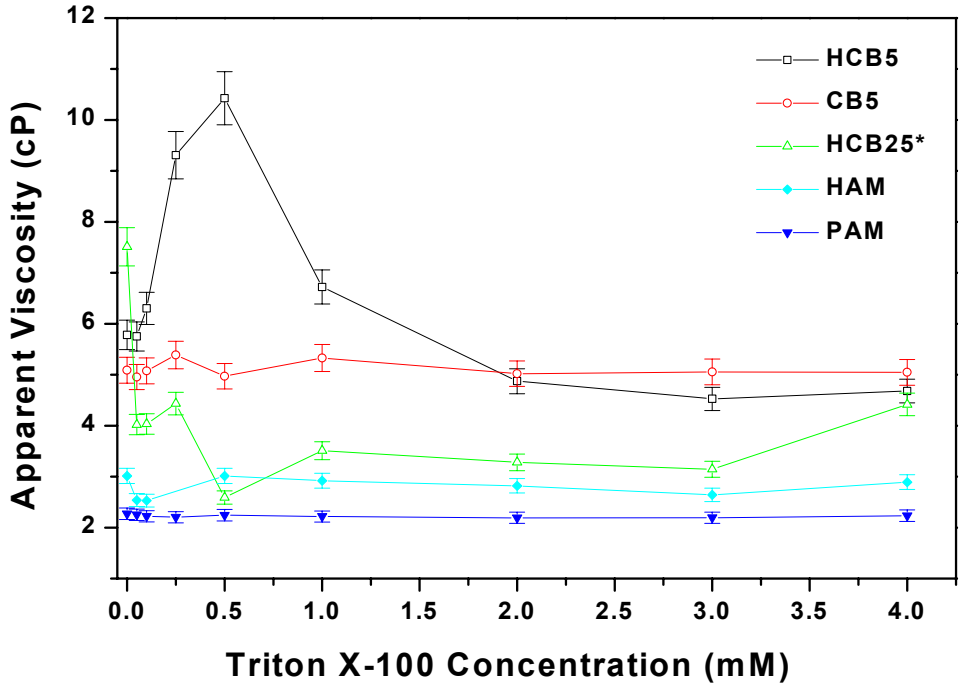

Figure 15. Apparent viscosity of the HM carboxybetaine terpolymers and the control polymers as a function of Triton X-100 concentration. Polymer concentration = 0.4 g/dL, except HCB25, polymer concentration = 0.1 g/dL, ambient pH (7.5 ± 0.5).

Interactions between the low charge density HM polybetaine terpolymers and control (co)polymers and surfactants were further probed using surface tension measurements. (The high charge density HM polybetaines HCB25 and HSB25 were not included in surface tension studies, as they did not demonstrate viscosity enhancement with any of the surfactants employed in the rheological studies) Surface tension profiles provide further evidence that PAM, SB5, and CB5 do not interact with Triton X-100. For example, the surface tension profiles shown in Figure 16 reveal that PAM and Triton X-100 do not interact, as indicated by the overlap of the two plots. However, crossovers of the surfactant-only trace and the polymer-surfactant traces are apparent in Figure 17, indicating that the HM polymers interact with Triton X-100 to form mixed micelles. HAM demonstrates even more unique behavior in the presence of Triton X-100: The lower surface tension values for Triton X-100 in the presence of HAM indicate that a surrface active complex is actually formed in solution. The surface tension values for Triton X-100 in the presence of HSB5 and HCB5 tend to be higher than those of HAM as a function of increasing Triton X-100 concentration. This may be due to a combination of slightly higher hydrophobe incorporation in the HM polybetaines and less surface activity due to betaine monomer incorporation.

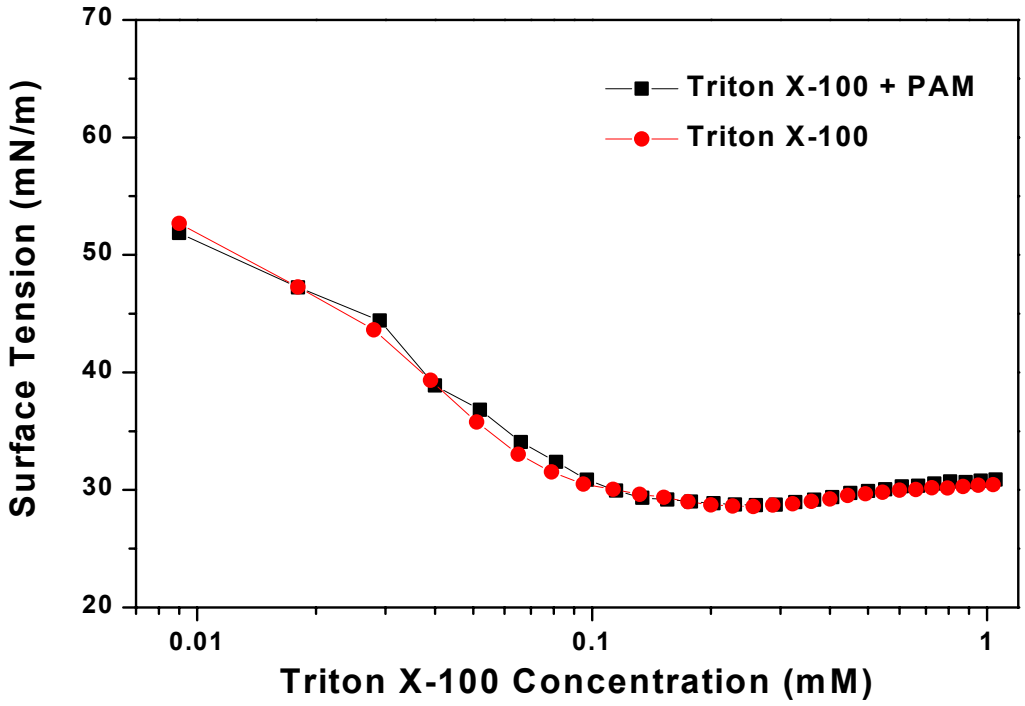

Figure 16. Plots of surface tension as a function of Triton X-100 concentration in the absence and presence of PAM homopolymer. PAM concentration = 0.2 g/dL, pH = 7.5 ± 0.5.

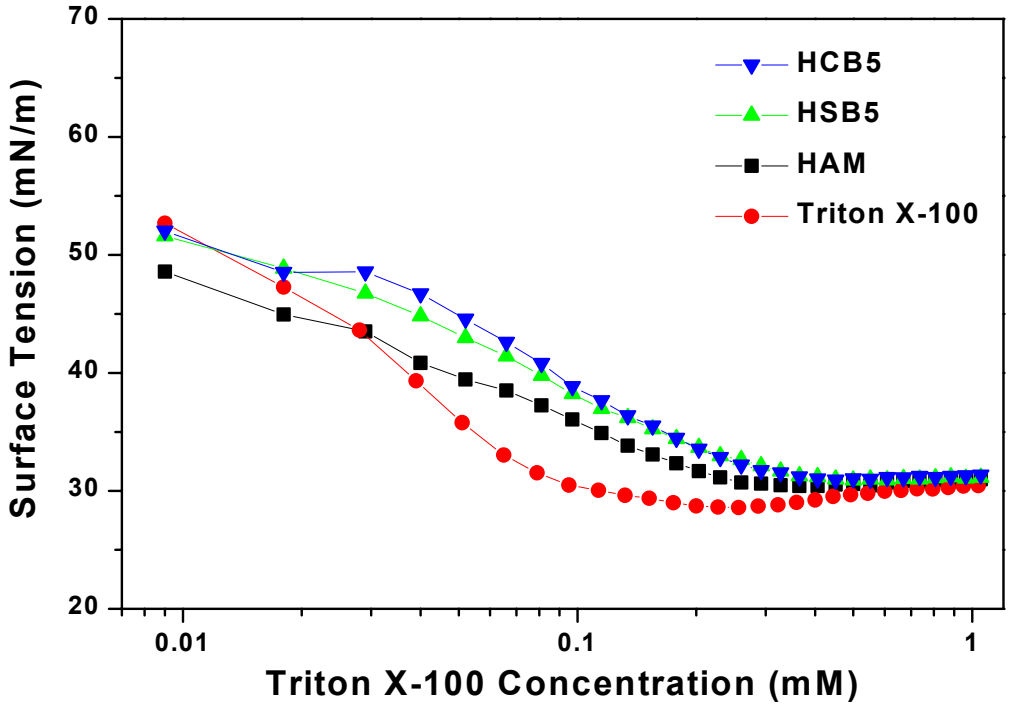

Figure 17. Plots of surface tension as a function of Triton X-100 concentration in the presence of low charge density HM polybetaines and the HAM control polymer. Polymer concentration = 0.2 g/dL, pH = 7.5 ± 0.5.

Effect of Zwitterionic Surfactant: The effect of the zwitterionic surfactant SB3-12 on the rheological behavior of HM polybetaines and control (co)polymers was also examined; the results are shown in Figures 18 and 19. HSB5, HCB5, and HAM are the only polymers that exhibit maxima in the plot of apparent viscosity as a function of SB3-12 concentration; this viscosity enhancement appears to be consistent with the model shown in Figure 11, Pathway 1. HCB5 displays a greater maximum in viscosity maximum than HSB5, as was the case for these polymers in the presence of Triton X-100. In the case of HCB25, SB3-12 addition causes a decrease in solution viscosity, most likely due to the disruption of intermolecular associations by the surfactant.

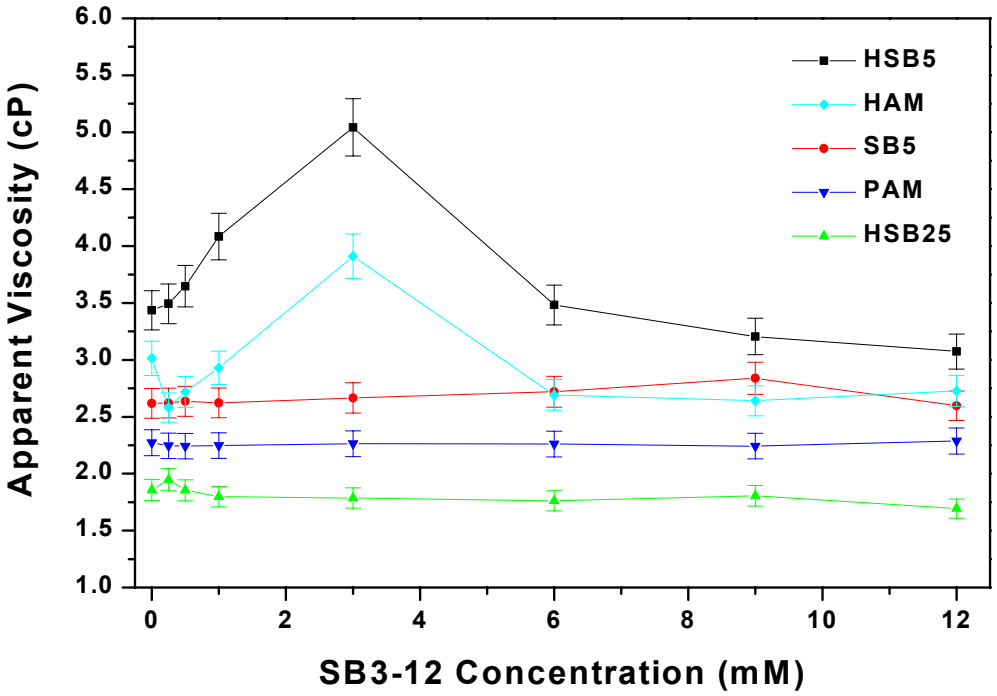

Figure 18. Apparent viscosity of the HM sulfobetaine terpolymers and the control polymers as a function of SB3-12 concentration. Polymer concentration = 0.4 g/dL, ambient pH (7.0 ± 0.5).

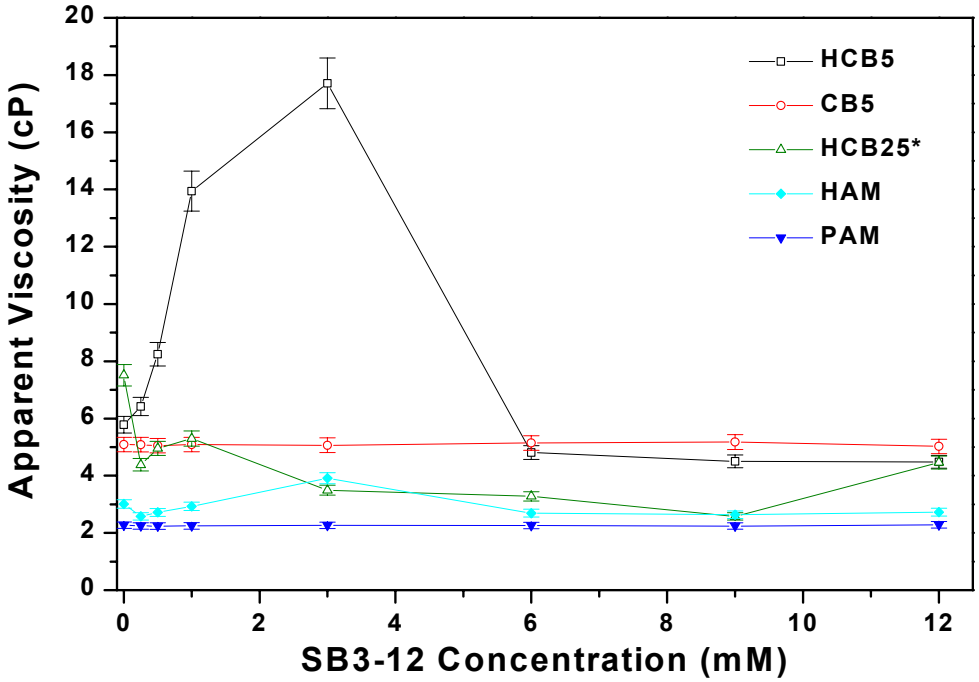

Figure 19. Apparent viscosity of the HM carboxybetaine terpolymers and the control polymers as a function of SB3-12 concentration. Polymer concentration = 0.4 g/dL, except HCB25, polymer concentration = 0.1 g/dL, ambient pH (7.0 ± 0.5).

Data from surface tension analysis (not shown) of these polymer-surfactant systems indicated a lack of interaction between non-HM polymers and SB3-12. As seen from the surface tension plots in Figure 20, all HM polymers investigated show indications of association with SB3-12. Two important conclusions can be drawn from the data in Figure 20: First, the lower surface tension values of SB3-12 in the presence of the HM polymers indicates that there is additive adsorption of polymer and surfactant at the air-water interface. Second, above the crossover concentrations (C_1 in Figure 12), the polymer-surfactant systems display characteristic comicellization in which the comicelles compete for surfactant with the air-water interface.

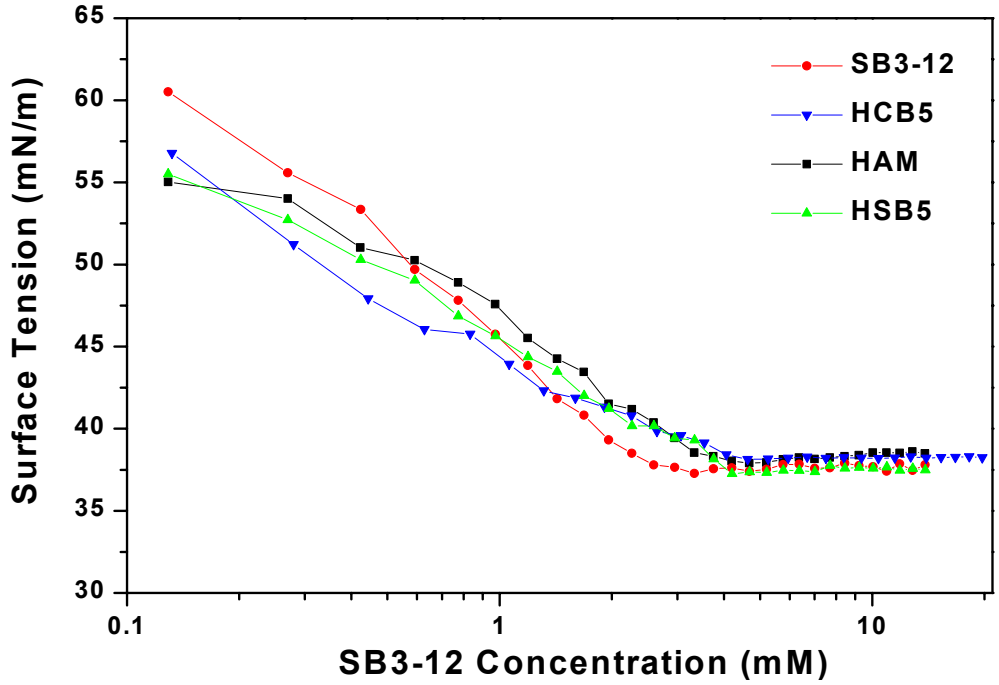

Figure 20. Plots of surface tension as a function of SB3-12 concentration in the presence of low charge density HM polybetaines and the HAM control polymer. Polymer concentration = 0.2 g/dL, pH = 7.5 ± 0.5.

Effect of Anionic Surfactant: Addition of SDS to aqueous polymer solutions had the most profound effect on solution viscosity enhancement. The viscosity responses of the HM polysulfobetaines and HM polycarboxybetaines to the addition of SDS are shown in Figures 21 and 22, respectively. Again, the HM polymers (HSB5, HCB5, and HAM) are the only samples to display viscosity maxima in the presence of SDS, with HCB5 exhibiting the greatest enhancement in viscosity upon SDS addition. The magnitude of the viscosity enhancement in the cases of HSB5, HCB5, and HAM caused by the addition of SDS is indicative of strong polymer-surfactant interactions. Given the highly cationic nature of the HM polycarboxybetaines at ambient pH, the polymer-surfactant interactions are probably a composite of hydrophobic and electrostatic interaction, especially in the case of HCB25, where precipitation is observed. This insolubility is consistent with data previously reported by Goddard and coworkers.[53]

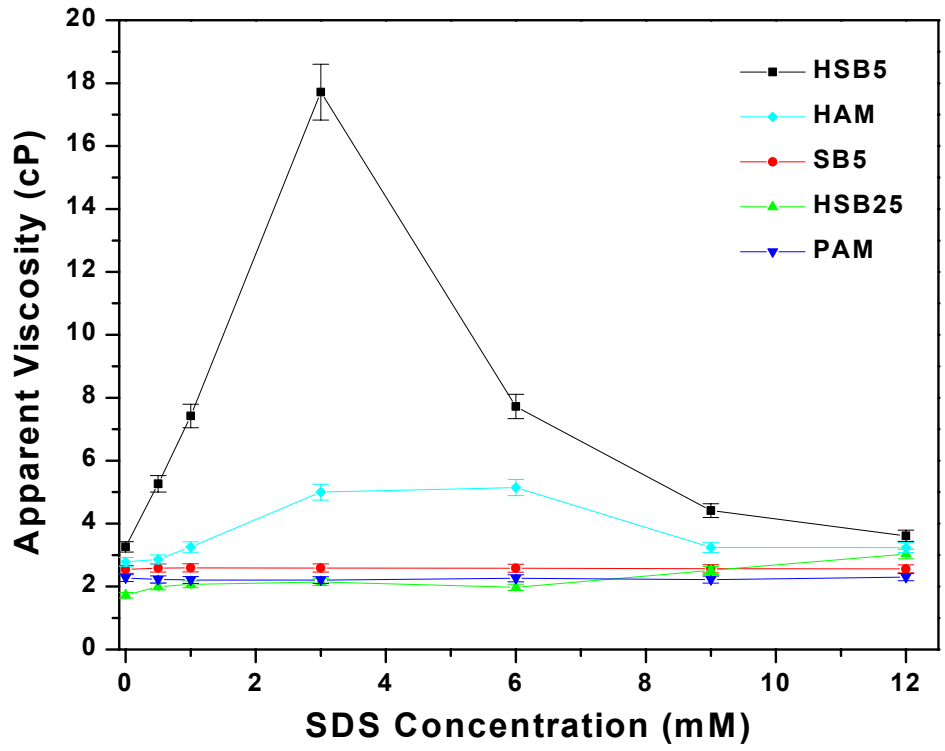

Figure 21. Apparent viscosity of the HM sulfobetaine terpolymers and the control polymers as a function of SDS concentration. Polymer concentration = 0.4 g/dL, ambient pH (7.5 ± 0.5).

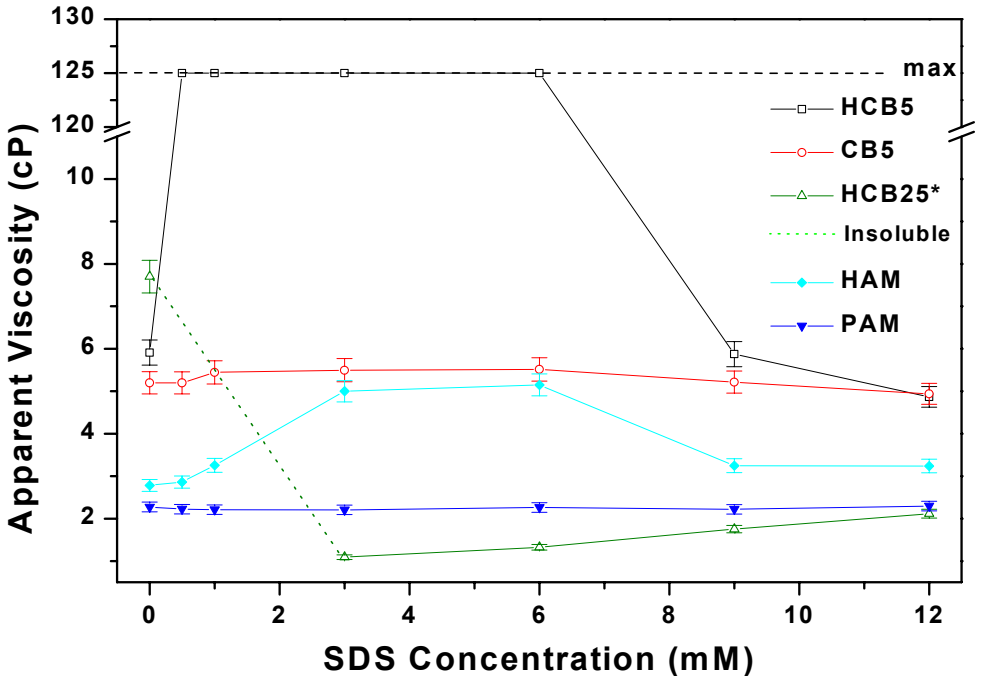

Figure 22. Apparent viscosity of the HM carboxybetaine terpolymers and the control polymers as a function of SDS concentration. Polymer concentration = 0.4 g/dL, except HCB25, polymer concentration = 0.1 g/dL, ambient pH (7.5 ± 0.5).

Data from surface tension experiments conducted to investigate the interaction between the HM polymers and SDS are shown in Figure 23. As in the previous cases, HAM, HBS5, and HCB5 show the characteristic features of polymer-surfactant interaction, while PAM, SB5, and CB5 do not (data not shown). Again, lower SDS surface tension values above C_1 in the presence of HM polymers indicate the formation of surface active polymer-surfactant complexes, and polymer-surfactant comicellization is apparent over the range of C_1 to C_2. The collective results from these surface tension studies demonstrate that hydrophobic modification of hydrophilic polymers is critical for surfactant-induced viscosity enhancement, regardless of whether or not betaine comonomers are employed.

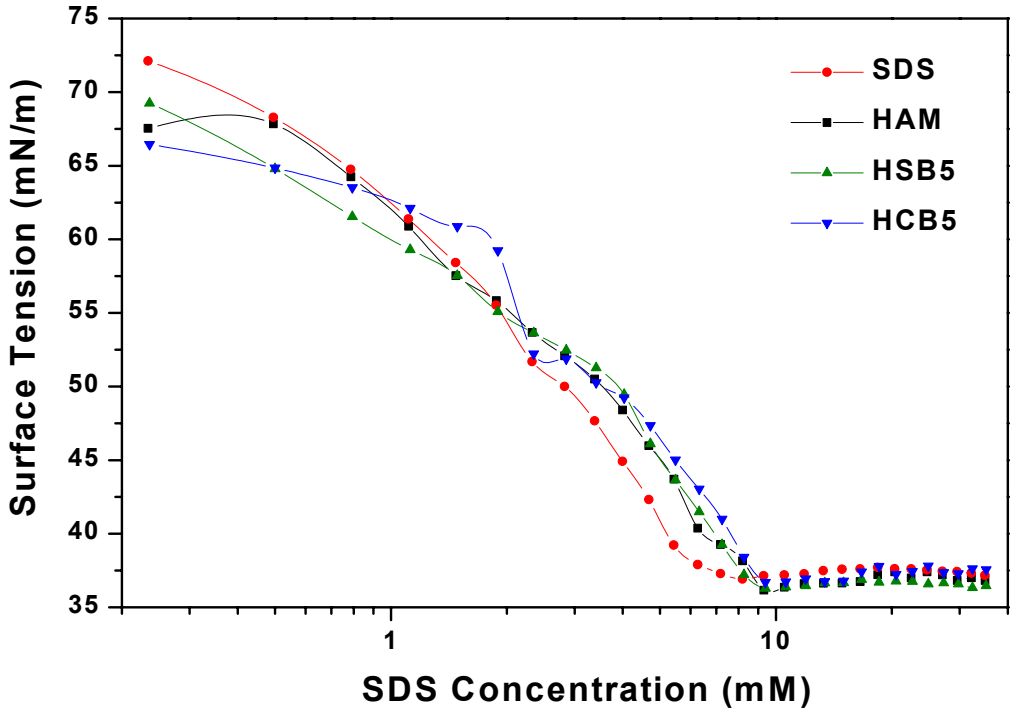

Figure 23. Plots of surface tension as a function of SDS concentration in the presence of low charge density HM polybetaines and the HAM control polymer. Polymer concentration = 0.2 g/dL, pH = 7.5 ± 0.5.

Effect of Cationic Surfactant: The solution behavior of the HM polybetaines and control (co)polymers was also investigated as a function of DTAB concentration, as shown in Figures 24 and 25. Consistent with the observed trend, HSB5, HCB5, and HAM all demonstrate viscosity maxima at an intermediate DTAB concentration, with HCB5 showing the greatest viscosity enhancement. It should be noted that significantly higher concentrations of DTAB are required to elicit viscosity enhancement compared to the polymer-surfactant solutions containing Triton-X-100, SB3-12, or SDS.

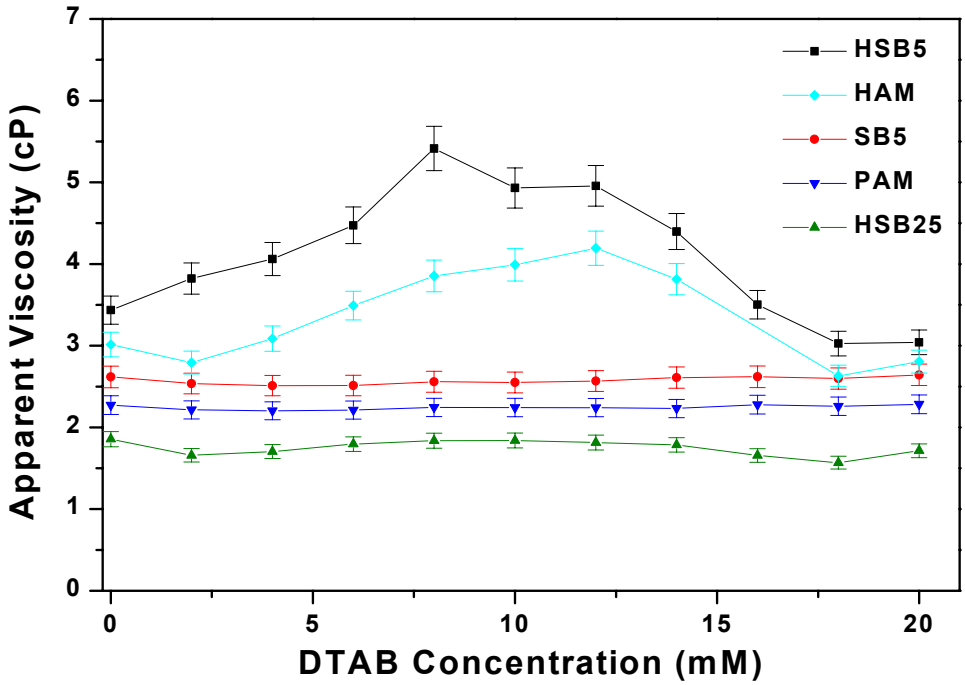

Figure 24. Apparent viscosity of the HM sulfobetaine terpolymers and the control polymers as a function of DTAB concentration. Polymer concentration = 0.4 g/dL, ambient pH (7.5 ± 0.5).

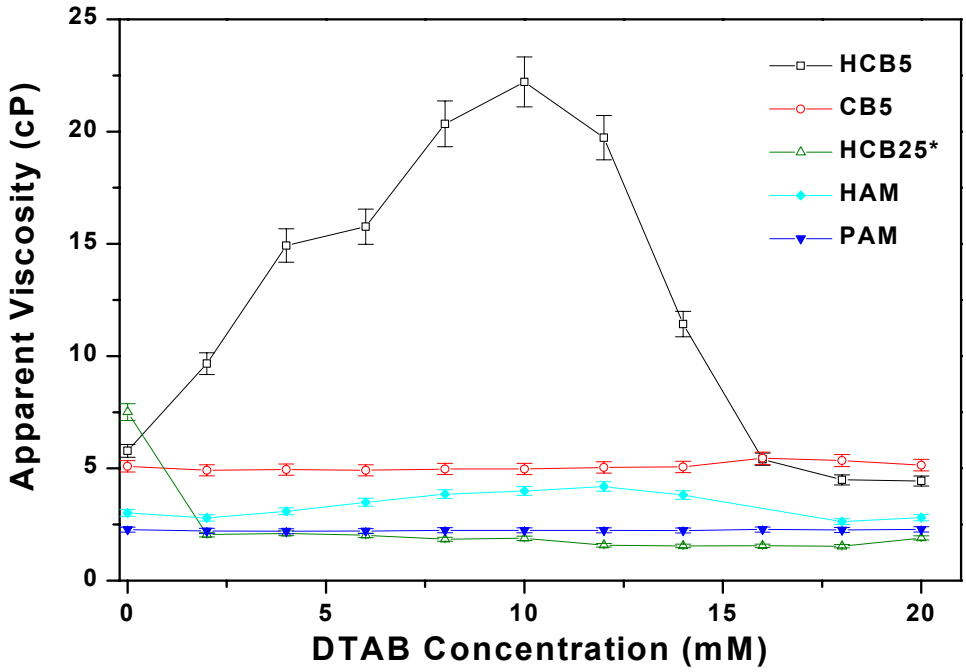

Figure 25. Apparent viscosity of the HM carboxybetaine terpolymers and the control polymers as a function of DTAB concentration. Polymer concentration = 0.4 g/dL, except HCB25, polymer concentration = 0.1 g/dL, ambient pH (7.5 ± 0.5).

The results of surface tension measurements conducted with DTAB and the polymers in this study are similar to those obtained from oppositely charged polymer-surfactant systems,[29,34,53,57] even in the case of PAM homopolymer (Figure 26). The interaction of PAM with DTAB was unexpected, as there was no apparent basis for interaction between PAM and DTAB, as was the case with PAM and Triton X-100 (Figure 16). We postulate that hydrolysis of the pendant amide groups may have occurred in the polymer samples to an extent not detected by NMR spectroscopy or potentiometry. It is reasonable to expect trace amounts of PAM hydrolysis during polymer synthesis, purification, and solution preparation/aging.[58] Interaction between the cationic ammonium headgroup of DTAB and the anionic carboxylate moieties along a partially hydrolyzed PAM chain may effectively bind hydrophobic groups to the chain, thus yielding a surface active complex, as seen in Figure 26. Due to the uncertainty introduced by the polymer hydrolysis issue, no quantitative information was obtained from the surface tension profiles in the presence of DTAB, as the exact mode of polymer-surfactant interaction could not be readily attributed to comicellization.

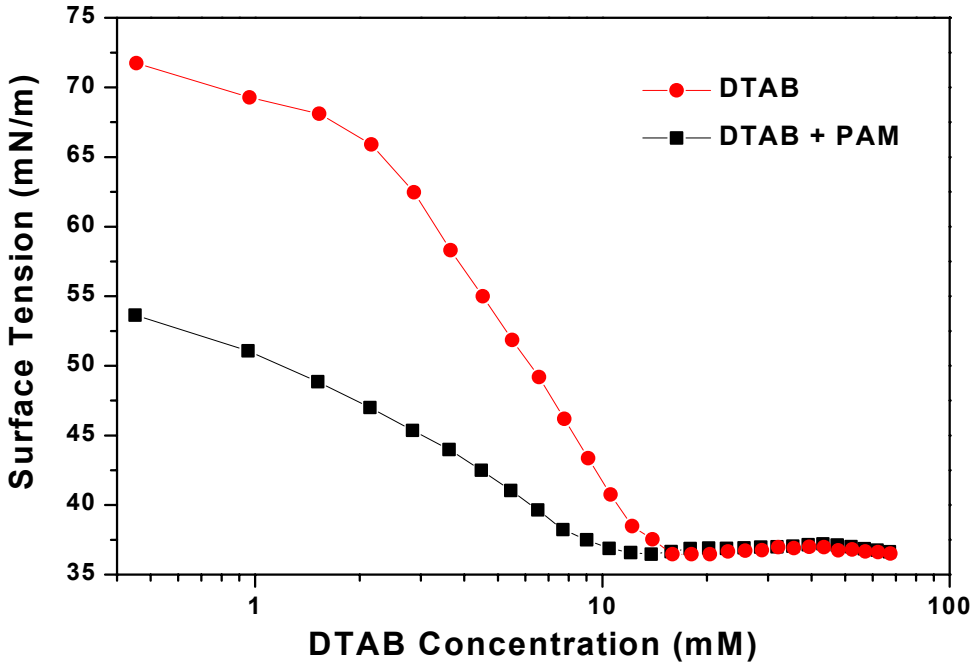

Figure 26. Plots of surface tension as a function of DTAB concentration in the absence and presence of PAM homopolymer. PAM concentration = 0.2 g/dL, pH = 7.5 ± 0.5.

Overall, SDS induces the largest changes in polymer solution viscosity, followed by DTAB and SB3-12, which have similar effects. Addition of Triton X-100 to polymer solutions results in little or no viscosity enhancement. The effect of surfactant headgroup on chain expansion and bridging is believed to be the reason for this trend. It is postulated that the microblocky architecture of the HM polymers induces hemi-micelle formation along the polymer backbone, resulting in chain expansion. This increased hydrodynamic volume allows coil overlap and thus hydrophobe exchange and insertion, resulting in bridged networks (Figure 11, Pathway 2). SDS apparently forms more effective networks with all of the HM polymers, followed by SB3-12, DTAB, and Triton X-100. This effect may be due to the nature of the hydration sphere around the mixed micelles that results in a balance between solubility and

bridging efficiency. The differences in the corona of mixed micelles from each of the surfactant types are likely to be significant, with headgroup charge and solvation playing major roles in intrachain conformation and interchain capture of hydrophobic units.

The nature of the interactions between HCB25 and most surfactants are such that viscosification mechanisms of this HM polycarboxybetaine (intermolecular hydrophobic and electrostatic association) are effectively inhibited. Unlike the other polymers, the addition of surfactant generally induces significant viscosity reduction in HCB25 solutions (Figures 15, 19, and 25), and precipitation is observed when small amounts of SDS are added to HCB25 solutions (Figure 22). The initial insolubility of HCB25, followed by its subsequent dissolution as additional SDS is added to the solution, is typical of oppositely charged polymer-surfactant interaction.[53] As stated previously, the pK_a of HCB25 is rather high and the polymer is predominately cationic at ambient pH; thus, SDS is strongly attracted to HCB25 due to combined electrostatic and hydrophobic interactions.

Polymer-Bound Surfactant: The onset of polymer-surfactant interaction is taken as the crossover point C_1 indicated in Figure 13. The point where surfactant micelle formation commences is called the saturation point, C_2. From C_2 and the *cmc* of the surfactant (cmc_{surf}), the number of bound surfactant molecules per polymer hydrophobe, *m*, can be calculated utilizing Equation 3, where [H] is the concentration of polymer-bound hydrophobes in mol/L.

$$m = \frac{C_2 - cmc_{surf}}{[H]} \tag{3}$$

Table 4. Values of C_1, C_2, and *m*, and derived from surface tension analysis.

Sample ID	C_1 (mM)	C_2 (mM)	*m*	Area/surfactant molecule (Å^2)
Triton X-100	—	—	—	46.3
HAM	0.018	0.73	3	94.3
HSB5	0.011	0.74	2.2	64.1
HCB5	0.011	0.67	2.5	62.4
SB3-12	—	—	—	45.5
HAM	0.59	4.2	5.7	57.1
HSB5	1.3	4.4	5.1	95.5
HCB5	0.92	4.2	5.5	80.2
SDS	—	—	—	12.1
HAM	0.5	9.4	8	28
HSB5	1.9	8.3	9.3	25.2
HCB5	1.1	9.4	8	27.5

Values of m were calculated in cases where C_1 and C_2 values could be obtained utilizing Equation 3. Due to the uncertainty in the nature of the polymer-DTAB interactions, data analysis was not performed on those surface tension profiles. Table 4 contains the values of C_1, C_2, and m obtained from the surface tension profiles. The parameter m tends to be higher for ionic surfactants. Values of m for Triton X-100 ranged from 2.2-3.0, and the range of m was observed to increase to 5.1-5.7 for SB3-12 and 8.0-9.3 for SDS. The lower values of m for Triton X-100 are expected, due to the greater size and irregular shape of this surfactant. Fewer Triton X-100 molecules are able to bind per hydrophobe as a result of the steric bulk of the ethoxylated headgroup and the non-straight chain hydrophobe.

Conclusion

A series of novel HM polysulfobetaine and polycarboxybetaine terpolymers were synthesized via micellar copolymerization along with corresponding control (co)polymers. The solution properties of the polymers were investigated as functions of various external stimuli, including changes in solution pH, electrolyte concentration, and the addition of small molecule surfactants. Results from rheological analysis indicate that low incorporations of sulfobetaine comonomer may promote intermolecular association above c^*, yet intramolecular associations prevail at high sulfobetaine comonomer incorporation. In addition to being non-pH-responsive, solutions of polysulfobetaines are relatively unaffected by the addition of NaCl. Carboxybetaine-containing polymers are more responsive, due in part to the cationic-favored charge imbalance present at ambient pH (as shown by potentiometric titration) and to the antipolyelectrolyte effect. The pH response of the polycarboxybetaines allows them to exhibit either PE, mixed PE/PZ, or PZ behavior depending on solution pH. The HM polycarboxybetaine containing a high betaine comonomer incorporation (HCB25) demonstrated anomalous solution behavior compared to the other polymers in this study, including extreme sensitivity to the addition of electrolytes and surfactants. It is postulated that this behavior is due to a complex interplay of hydrophobic interactions, hydrogen bonding, and electrostatic interactions that may lead to reversible aggregate formation in solution.

The low charge density HM polybetaines and the nonionic HAM copolymer were shown to interact with surfactants, as demonstrated by rheological and surface tension analyses. Changes in polymer solution viscosity upon addition of surfactant are consistent with the conceptual model shown in Figure 11, although the the degree of surfactant-induced viscosity enhancement is widely varied depending on surfactant type. SDS was found cause the most profound viscosity enhancement, followed by SB3-12, DTAB, and Triton X-100. Headgroup ionic effects and hydration are believed to account for the observed trend. Surface tension experiments generally corroborate the evidence of surfactant-polymer interactions derived from rheological analysis, although the surface tension profiles of polymer-DTAB interactions are anomalous and require further investigation.

TASK 5: *Polymer Solution Mobility*

Viscosity Behavior of Polyelectrolyte Solutions

Experience has shown that efficient polymers for oil recovery must have a large hydrodynamic coil size in solution as they flow through the reservoir. Larger polymer coils have higher extensional viscosities, which lower aqueous phase mobility in the porous media, and thereby improve sweep efficiency to displace residual reservoir oil.

Ideally, the macromolecules should have a collapsed coil configuration during injection into the reservoir to reduce both pumping costs and shear degradation at the well-head. Also, polymer coils should expand after injection to increase their solution extensional viscosity within the reservoir. The desired complex solution behavior may be achieved with synthetic polymers that can change their macromolecular conformation upon encountering certain environmental stimuli such as variations in solution temperature, pH, and electrolyte concentration.

In our last report, we discussed solution thermodynamic theory that described changes in polymer coil conformation as a function of solution temperature and polymer molecular weight.[59] These polymers contained no ionic charges. In this report, we expand polymer solution theory to account for the electrostatic interactions present in solutions of charged polymers. Polymers with ionic charges are referred to as polyions or polyelectrolytes.

Polyelectrolytes

Polyelectrolytes are macromolecules that have ionizable groups distributed along the polymer chain. When dissolved in water, the ions dissociate, and charges are formed on the polymeric backbone. Polyelectrolytes can be cationic or anionic. A polycation can be formed when a polybase (i.e. a polyamine) is dissolved in water. The functional group can bind a proton, yielding a positively charged functionality and a negative hydroxyl counterion. A polyanion is produced when a polyacid is dissolved in water causing dissociation of the acid group to a negative functionality and a positive hydronium counterion. In either case, the ion dissociation is an equilibrium-controlled process in which the extent of dissociation, and thus the number of charged groups on the backbone, can be manipulated by adjusting the solution pH. A polyampholyte is a polymer that contains both acidic and basic functionalities along its backbone, in which case the proportion of positive and negative charges depends on the solution pH. Polyelectrolytes can also be polysalts, which, upon dissolution in water, dissociate into polyions and corresponding counterions.

As illustrated in Figure 27, a polyelectrolyte solution contains polyions, their counterions, and, often, other ions from added salts.[60] All charged species except those bonded to the polymer chain are considered mobile ions in the solution. The charged groups on a polyelectrolyte differ from the mobile ions because they are covalently linked together by the polymer backbone and, therefore, do not have mobility within the solution. Coulombic electrostatic forces among polyion charges and mobile solution ions greatly influence the polyelectrolyte solution properties. The existence of charges on the polymer leads to intra- and

inter-macromolecular interactions, which may be stronger and of much longer range than interactions of uncharged macromolecules. The degree of interaction between charges on a polyion depends strongly on the distance between the charges along the polymer. Therefore, an important parameter affecting polyelectrolyte solution behavior is the spatial distribution of charges along the polymer backbone.

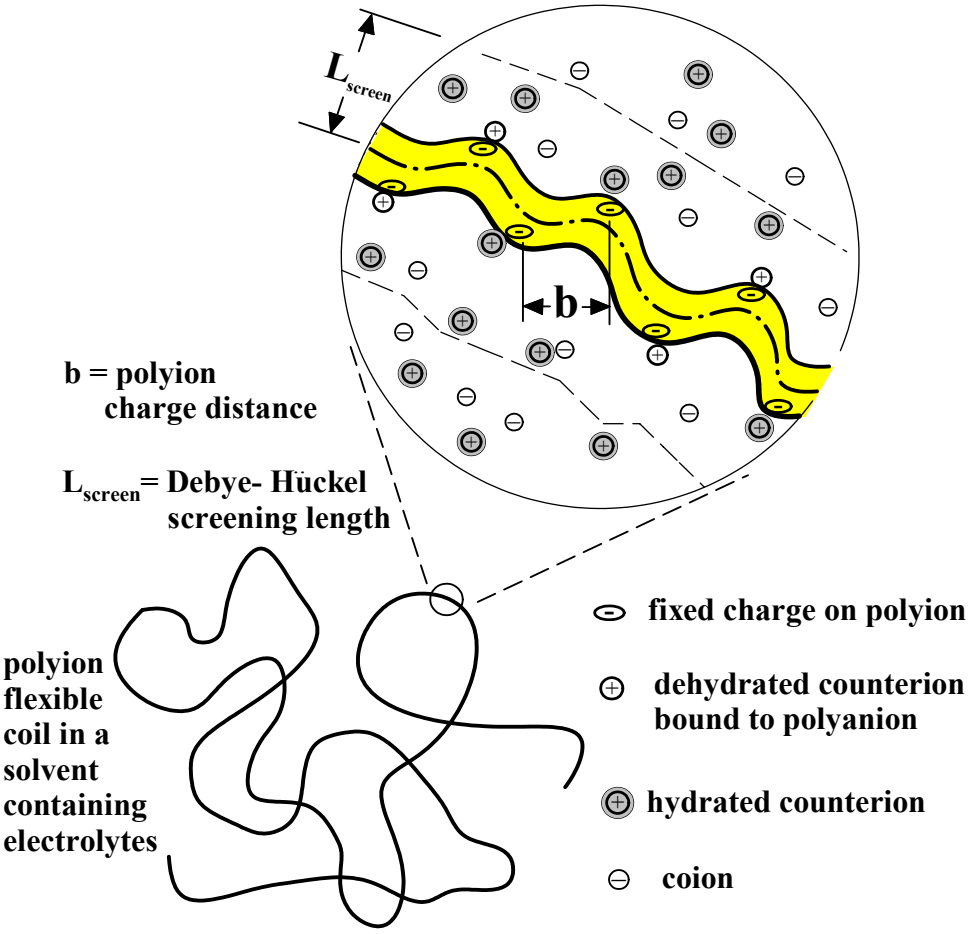

Figure 27: Schematic of Polyion in a Salt Solution

Polyion Charge Spacing

The distance between charges on a polyelectrolyte, b, can be controlled in several ways. Illustrations in this section depict polymers for which experimental data from the literature is analyzed in a later section of this report.

Figure 28a shows a copolymer composed of a neutral monomer and a charged comonomer (in this case acrylamide and (N,N,N-trimethyl)amionoethyl chloride, respectively). In this example, the charge spacing, b, is inversely proportional to the amount of the ionizable comonomer included in the polymerization. Thus, b can be controlled synthetically.

Another commonly encountered synthetic method for controlling charge spacing is post-polymerization hydrolysis, specifically of poly(acrylamide). Figure 28b shows a partially hydrolyzed poly(acrylamide) or HPAM. The extent or degree of hydrolysis of the neutral amide functionality to an ionizable acid (or salt, depending on reaction conditions) determines the resulting polyelectrolyte charge spacing, in similar fashion to the copolymerization method.

Another example of polymer modification to a polyelectrolyte is conversion of cellulose to sodium carboxymethly cellulose or NaCMC (see Figure 28c). The charge spacing depends on the degree of substitution, which is defined as the number of ionizable groups per glucose ring.

Finally, charge spacing in polyacids and polybases can be controlled by changing the pH. For example, a fraction of the negatively charged groups on poly(acrylic acid), or PAA (see Figure 28d), can be protonated by lowering the solution pH. Lowering the pH will reduce the number of charges on the polyion, thus increasing the charge spacing, until eventually the polymer becomes uncharged. This is an example of a polymer system whose flow behavior can be manipulated using solution pH as a stimulus to alter polyion charge spacing.

In all of the methods listed above, the fraction of charged repeat units determines the number of neutral repeat units separating the charges, and, thus, the charge spacing. Adjusting the charge spacing is one way of controlling polyelectrolyte coil conformation and coil size in solution and thereby gives a method to tailor solution flow properties for specific applications.

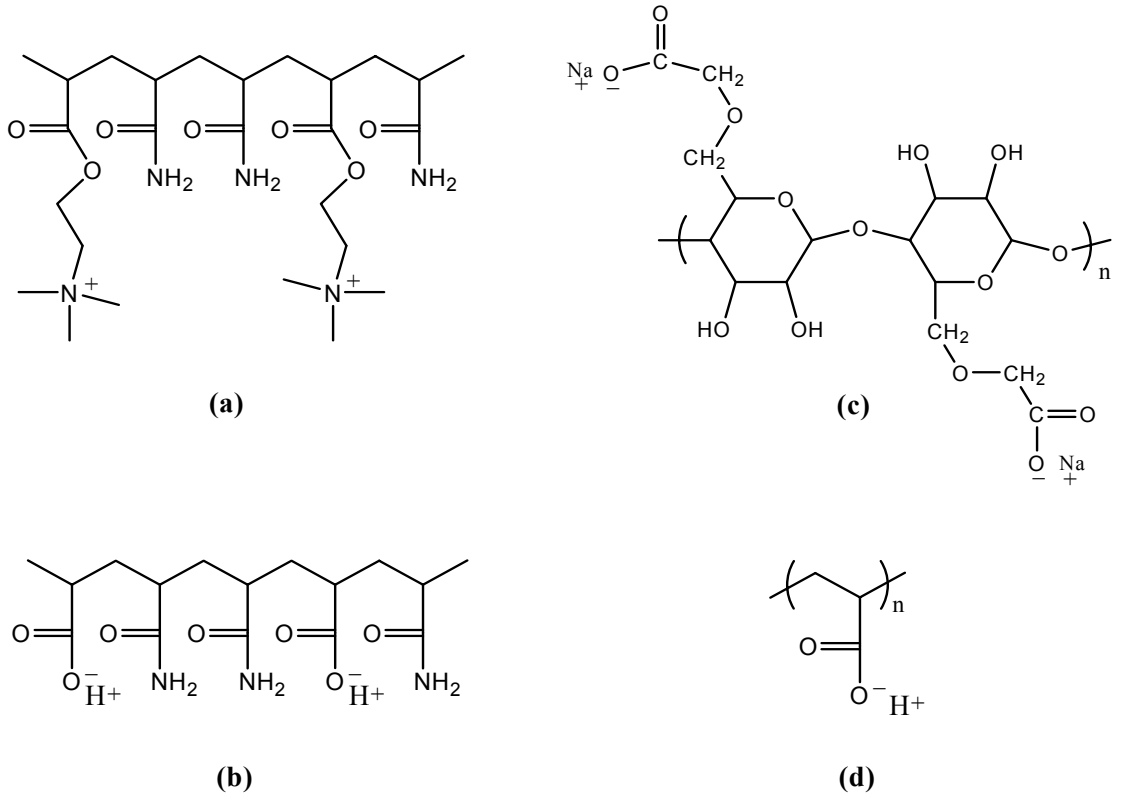

Figure 28: Examples of Polyelectrolytes. (a) representative section of poly(acrylamide-co-(N,N,N-trimethyl)amionoethyl chloride. (b) section of partially hydrolyzed poly(acrylamide).

(c) repeat unit of sodium carboxymethyl cellulose with degree of substitution of 1. (d) repeat unit of poly(acrylic acid).

Polyelectrolyte Solution Parameters

Scientists have defined several parameters that can be used to describe the environment existing within polyelectrolyte solutions. These parameters include solution ionic strength, the Bjerrum length, the Debye-Hückel screening length, and the Manning parameter.

Solution Ionic Strength

The ionic strength of a polyelectrolyte in a salt solution, I, results from the *mobile ions* present in the solution. This includes all the salt cations and anions present and the mobile counterions associated with the immobile charges attached to the polyion. The mathematical definition for the solution ionic strength is given by

$$\mathbf{I = \frac{1}{2} \bullet \left[Z_p \bullet z_p^{\,2} \bullet C_{polymer} + \sum_i \left(z_i\right)^2 \bullet C_{salt_i} \right]} \qquad \mathbf{(1)}$$

In the above relationship Z_p is the number of charges on a single polyion (equal to the number of polymer counterions), z_p is the charge valence of the polymer counterions, $C_{polymer}$ is the polymer molar concentration, z_i is the charge valence of salt ion i and C_{salti} is the molar concentration of salt ion i.

Bjerrum Length

The Bjerrum length, l_B, is the distance between two identical charges in a medium at which the electrostatic and thermal energies are equal. Thus, the Bjerrum length is a measure of the strength of charge-charge interaction in a medium. At 25 ^oC the Bjerrum length for water is 7.14 Å. The Bjerrum length can be calculated using Equation (2) at absolute temperature T for any medium having a dielectric strength ε.

$$\mathbf{l_B = \frac{elec^2}{4 \bullet \pi \bullet \varepsilon_o \bullet \varepsilon_r \bullet k_B \bullet T}} \qquad \mathbf{(2)}$$

Equation (2) contains three constants, ε_o, the permittivity of a vacuum, 8.85 x 10^{-12} coul^2 per (Newton meter^2), k_B, the Boltzmann's constant, 1.380 x 10^{-16} erg per K, and elec, the charge of an electron, 1.602 x 10^{-19} coul. A medium's dielectric strength, $\varepsilon = \varepsilon_r\ \varepsilon_o$, is inversely proportional to its ability to transmit electrostatic forces between charges; i.e., with all other conditions constant, a medium with a higher dielectric strength will transmit less electrostatic force than a medium with a lower dielectric strength. For a water medium, the relative permittivity, $\varepsilon_r = \varepsilon / \varepsilon_o$, is a function of the temperature, t, in ^oC, as shown by relationship below.[61] At 25 ^oC, ε_r for water is 78.54.

$$\varepsilon_r = 78.54 \bullet \left[1 - 5.58 \bullet 10^{-3} \bullet (t - 25) + 1.19 \bullet 10^{-5} \bullet (t - 25) - 2.8 \bullet 10^{-8} \bullet (t - 25) \right]$$

The dielectric strength, ε, is the property of the medium surrounding the charges that affects the force between the charges. ε is found in Coulomb's law which gives the force, F, between two electrostatic charges, Q and Q', separated by a distance, s.

$$F = \frac{Q \bullet Q'}{4 \bullet \pi \bullet \varepsilon \bullet s^2} = \frac{Q \bullet Q'}{4 \bullet \pi \bullet \varepsilon_r \bullet \varepsilon_o \bullet s^2} = \frac{Q \bullet Q'}{D \bullet s^2}$$

The product, $4 \bullet \pi \bullet \varepsilon_r \bullet \varepsilon_o$, is defined as the medium's dielectric constant, D.

Debye-Hückel Screening Length

The Debye-Hückel screening length is a measure of the distance over which a charge can exert an electrostatic force. The screening length represents the thickness of the ionic atmosphere surrounding a charge placed in a medium. As the distance between adjacent polyion charges become progressively larger than the screening distance, the repulsive forces between the polymer charges approach zero. Because polymer ions tend to surround themselves with an atmosphere of oppositely charged ions, the screening length decreases as the solution ionic strength increases. The Debye-Hückel screening length, L_{screen}, can be calculated using Equation (3).

$$L_{screen} = \sqrt{\frac{\varepsilon_r \bullet \varepsilon_o \bullet k_B \bullet T}{2 \bullet N_A \bullet elec^2 \bullet I}} \qquad (3)$$

Manning Parameter

As the distance between charges on a polyion decreases and begins to approach the Bjerrum length, counterions surrounding the polymer condense onto the polymer charges and begin to reduce the effective charge density along the polyion. Manning's parameter, ξ, is the ratio of the Bjerrum length, l_B to the polyion charge spacing, b, i.e., $\xi = l_B / b$. For a stable solution, Manning showed that this parameter can never exceed unity.[62] Therefore, the effective spacing between adjacent polyion charges can never be less than the Bjerrum length. Recall that the Bjerrum length for water at 25 ^oC is 7.14 Å.

Polyelectrolyte Solution Intrinsic Viscosities

The intrinsic viscosity of a non-ionic polymer in solution is determined by measuring the fluid viscosities of dilute polymer solutions over a range of polymer concentration. Solution reduced viscosities, η_{red}, are calculated by comparing solution viscosities, η_s, to the solvent viscosity, η_o, as given in the following relationship where C_p is the polymer concentration.

$$\eta_{red} = (\eta_s - \eta_o) / (\eta_o C_p)$$

A reduced viscosity is thus calculated for each polymer solution concentration. The intrinsic viscosity is the linear extrapolation of the reduced viscosity to a polymer concentration of zero.

Due to complications arising from charge interactions in polyelectrolyte solutions, the intrinsic viscosity of a polyelectrolyte solution is difficult to accurately determine. Polyelectrolyte solution intrinsic viscosity cannot be determined by the treatment just described for non-ionic polymers, because a plot of reduced viscosity versus concentration for polyelectrolyte solutions does not yield a straight line. At low polyelectrolyte concentrations, solution reduced viscosity increases drastically as concentration decreases, a behavior known as the "polyelectrolyte effect". A linear extrapolation is therefore impossible. Nonlinear extrapolations have been used in the past to determine polyelectrolyte intrinsic viscosities, but more recent theory has shown that such methods are not always accurate.

The underlying cause of the "polyelectrolyte effect" is that the solution ionic strength is not constant when a range of polyelectrolyte concentrations is prepared. Intrinsic viscosity is a measure of the polymer coil size in solution, which depends on the solution ionic strength. Thus, an accurate intrinsic viscosity determination requires that each polyelectrolyte solution have the same ionic strength. Appreciable portions of the mobile ions that determine the solution ionic strength come from the polymer itself. At a given salt concentration, solutions containing less polymer have lower ionic strength. Therefore, the dilute polymer solutions must be prepared by the method of isoionic dilution. In this method, the more dilute solutions, where less polymer counterions are present, are made to have a constant ionic strength by adding an appropriate amount of salt, such as sodium chloride.

Several methods of performing isoionic dilution are conceivable, but for the purposes of our experimentation the following practical procedure will be employed. A "stock" solution in deionized water is prepared having a relatively high polymer concentration and a calculated amount of added salt, so that the solution ionic strength equals the desired experimental value. A second "solvent" solution of salt in deionized water is prepared such that its ionic strength is equal to that of the stock polymer solution. Note that the solvent solution will have a slightly higher salt concentration to account for the absence of the mobile polyelectrolyte counterions. Portions of the stock solution are then diluted by adding appropriate amounts of the solvent solution to yield the desired polymer concentrations for intrinsic viscosity determination. Assuming that volume is additive (justifiable for aqueous solutions of similar composition), the ionic strength of the resulting solutions, in moles of ions per liter of solution, will be the same no matter the extent of dilution. When a set of solutions having a range of polymer concentrations

is prepared in this manner, the ionic strength will be constant for all solutions, and a plot of reduced viscosity versus concentration should be linear.

When determining solution ionic strengths, one must be aware that polyelectrolyte solutions contain sources of ions, other than the polymer and added salt, that may become significant at low ionic strength. When calculating solution ionic strength, the numbers of ions due to added biocide (i.e., 50 ppm sodium azide, NaN_3) and the auto-ionization of water must be considered. The quantity of ions from such sources, however, should be very nearly equal in the stock and solvent solutions. Therefore, the method described above for maintaining constant ionic strength remains valid, even in the limit of very low ionic strengths.

Polyelectrolyte Solution Theory

Many theoretical analyses have been performed in the past; however, to date no theory is capable of adequately explaining all polyelectrolyte solution properties at all possible solution conditions. We will limit our discussion to the polyelectrolyte theories that apply to determining the viscosity of aqueous dilute solutions of flexible coil polyions containing low molecular weight ionizable salts, such as sodium chloride. These are the solutions that exist when using polymer to flood oil reservoirs.

Scaling Theory

Rubinstein[63] and other[64] have used the scaling concepts introduced by de Gennes[65] with a wormlike polymer chain model to theoretically investigate polyelectrolyte solution behavior. The wormlike polyelectrolyte chain is pictured as a random coil of connected blobs. Each identical blob is made up of a finite number of monomer units and can be considered to have a radius that depends upon polymer structure and solvent properties. Within a blob, only internal electrostatic forces are present. Results from this work can be used to predict many polyelectrolyte properties in salt solutions.

Polymer Conformation in Dilute Solutions

Scaling theory shows that polyelectrolytes in dilute solutions will convert from flexible coil conformations into rigid, rod-like structures when the number of salt ions becomes less than the number of charges on the polymer. A flexible polymer coil conformation is assured when the concentration of salt in the solution, C_{salt}, is greater than 10 times the product of the polymer concentration, $C_{polymer}$, and the number of charges on a single polymer, Zp. Therefore, the minimum salt concentration to assure a flexible polymer coil conformation, C_{sMin}, is given by Equation (4). This stipulation is referred to as the excess of salt condition.

$$\mathbf{C_{sMin} = 10 \bullet Z_p \bullet C_{polymer}} \qquad \mathbf{(4)}$$

Polymer Coil Overlap

Polymer dilute solution conditions exist only when individual polymer coils do not interact or have overlapping domains. Thus, polymer concentrations must not exceed a specific concentration if dilute solution conditions are desired. The polymer concentration at the overlap condition is denoted C_{pStar}. Usually C_{pStar} is the polymer concentration existing when the

solution viscosity is approximately twice the solvent viscosity. Scaling theory suggests that the C_{pStar} value for a polyelectrolyte in a salt solution is given by Equation (5).

$$C_{pStar} = \left(\frac{2^{21} \bullet C_{salt}{}^{21} \bullet m_o{}^{18}}{N_A{}^{14} \bullet Z_p{}^{45} \bullet M^{18} \bullet b^{30} \bullet l_B{}^{12}} \right)^{\frac{1}{35}} \qquad (5)$$

In Equation (5), m_o is the molecular weight of the monomer unit, M is the polymer molecular weight, b is the average distance between charges on a polyion, l_B is the Bjerrum length and N_A is Avogadro's number, 6.02×10^{23} per mole.

When polyelectrolyte solution intrinsic viscosity measurements are performed, solution conditions for all fluid viscosity measurements must be made such that polymer flexible coil conformations are always present in the solution and that polymer concentrations are below the overlap polymer concentration, C_{pStar}. These experimental restrictions are sometimes difficult to satisfy, but are essential to obtaining intrinsic viscosity information that is correct and meaningful.

Odijk, Skolnick, Fixman (OSF) Theory

In this theoretical treatment[66,67] the polyelectrolyte was treated as an unstructured, charged space curve (a wormlike polymer) with a continuous charge distribution having no fluctuations due to thermal motion. A persistence length was determined for polymers that are locally stiff such that excluded volume effects are negligible. This condition usually exists for low ionic strength solutions of polyions near theta solvent conditions. Given these restrictions, the electrostatic persistence length, q_e, was determined as

$$q_e = \frac{l_B}{4} \bullet \left(\frac{L_{screen}}{b} \right)^2 \qquad (6)$$

Equation (6) applies only to locally stiff polyions. As indicated by Equation (7), polyions are stiff when the average spacing between charges on a polymer, b, is less than the square root of the product of the polymer's persistence length in the absence of electrostatic effects, q_o, and the Bjerrum length, l_B.[64] In most cases of practical interest, polyelectrolytes in salt solutions are not locally stiff. Thus, Equation (6) is not applicable for most polyions in salt solutions.

$$b < \sqrt{q_o \bullet l_B} \qquad (7)$$

Modified OSF Theory

For wormlike flexible polymers, Yamakawa[68] developed a relationship between the intrinsic viscosity, η_{intr}, and the persistence length, q. The intrinsic viscosity is a measure of the average polymer coil size existing in the solution. The persistence length serves as a measure of the effects of short-range solvent and polymer interactions on the conformation of a polymer chain. As shown by Equation (8), the intrinsic viscosity is proportional to the polymer's persistence length to the 1.5 power. In Equation (8), l_m is the length of a monomer unit in the polymer chain, and Φ_o is the Flory constant for non-draining, flexible polymer coils and is equal to 2.86×10^{23} mole^{-1}.

$$\eta_{intr} = \left(\frac{2 \bullet l_m}{m_o}\right)^{\frac{3}{2}} \bullet \Phi_o \bullet M^{\frac{1}{2}} \bullet q^{\frac{3}{2}} \qquad (8)$$

For polyelectrolytes in solution, Fixman[66] has suggested that the total persistence length, q, can be considered as the sum of a persistence length due to electrostatic repulsion forces between polyion charges, q_e, and the persistence length in the absence of electrostatic effects, q_o. Using this sum for q in Equation (8) with rearrangement gives Equation (9).

$$\eta_{intr}^{\frac{2}{3}} = \frac{2 \bullet l_m}{m_o} \bullet \Phi_o^{\frac{2}{3}} \bullet M^{\frac{1}{3}} \bullet q_o + \frac{2 \bullet l_m}{m_o} \bullet \Phi_o^{\frac{2}{3}} \bullet M^{\frac{1}{3}} \bullet q_e \qquad (9)$$

The first term on the right side of Equation (9) must be the solution intrinsic viscosity to the 2/3 power when electrostatic effects are not present, i.e., when q_e equal to zero. At very high electrolyte or salt concentrations, electrostatic repulsion forces between charges on a polyion become insignificant due to polymer charge screening by the abundance of solvent salt ions. Thus, the intrinsic viscosity at high salt solution conditions, η_{intrHS}, can be used determine the first term on the right side of Equation (9) and results give Equation (10)

$$\eta_{intr}^{\frac{2}{3}} = \eta_{intrHS}^{\frac{2}{3}} + \frac{2 \bullet l_m}{m_o} \bullet \Phi_o^{\frac{2}{3}} \bullet M^{\frac{1}{3}} \bullet q_e \qquad (10)$$

OSF theory predicts that the electrostatic persistence length for stiff polyions is given by Equation (6). In this relationship q_e is proportional to the screening length, L_{screen}, to the second power. However, this dependence is only valid for stiff polymers.[69] For flexible polymers, experimental data from many laboratories[70-72] have shown that the persistence length is directly proportional to the screening length to the first power. Therefore Equation (11), which reflects this experimental finding and is similar to Equation (6), will be used for the persistence length of flexible polymers.

$$q_e = k \bullet \frac{l_B}{4} \bullet \left(\frac{L_{screen}}{b} \right) \qquad (11)$$

In Equation (11), b is the distance between polyion charges and k is a constant of proportionality. Combining Equations (10) and (11) gives Equation (12).

$$\eta_{intr}^{\frac{2}{3}} = \eta_{intrHS}^{\frac{2}{3}} + \frac{2 \bullet l_m}{m_o} \bullet \Phi_o^{\frac{2}{3}} \bullet M^{\frac{1}{3}} \bullet k \bullet \frac{l_B}{4} \bullet \left(\frac{L_{screen}}{b} \right) \qquad (12)$$

Equation (12) can be arranged to give Equation (13). The left side of Equation (13) contains parameters related to the polymer solution intrinsic viscosities and polymer structure. The left side of Equation (13) can be the ordinate for plotting experimental data. The right side of Equation (13) contains a set of constants multiplied by the ratio of screening length to the average spacing between adjacent charges on the polyion. The ratio of screening length to the average spacing between charges on the polyion can be the abscissa for plotting data.

$$\left(\frac{\eta_{intr}^{2} - \eta_{intrHS}^{2}}{M} \right)^{\frac{1}{3}} \bullet \frac{m_o}{l_m} = \frac{k \bullet l_B \bullet \Phi_o^{\frac{2}{3}}}{2} \bullet \left(\frac{L_{screen}}{b} \right) \qquad (13)$$

Polyelectrolyte solution experimental data is typically collected as intrinsic viscosity values versus solution ionic strengths. In most cases polymer molecular weight, monomer unit molecular weight, and monomer length are known. With this knowledge, experimental data can be plotted in a manor corresponding to Equation (13). Equation (13) predicts that the plotted data will fall on a straight line with a zero intercept. The slope of this plotted data should be equal to $(k\ l_B\ \Phi o^{2/3}) / 2$. If Equation (13) is consistent with experimental data, all polyelectrolyte solution experimental data, regardless of polymer type or molecular weight, should fall on a single straight line.

Polyelectrolyte Solution Data

Four sets of polyelectrolyte data were selected from the scientific literature. This data contained the necessary information to test the validity of Equation (13). Three data sets are for polyanions, and one data set is for a polycation. All data sets have known polymer molecular weights, polyion structures, and solution intrinsic viscosity values measured over a range of aqueous solution ionic strengths using sodium chloride salt. The properties of each data set and the solution data are given in Table 5.

All polyelectrolyte solution intrinsic viscosities taken from the scientific literature were determined using salt solutions so chosen such that the ionic strength of all solutions used to find

a single intrinsic viscosity value were constant. This experimental technique used to find polyelectrolyte solution intrinsic viscosities, the isoionic dilution method, was described above.

The average polyion charge spacing, b, for each polyelectrolyte was determined by using Chem3D Ultra, a computer software package that minimizes molecular structure conformational energies. After polymer conformational energies were minimized, the spacing between charges was averaged to give b. These values are reported in Table 5.

The polyelectrolyte charge spacing can also be determined by multiplying the average number of monomer units between polymer charges by the monomer length in the polymer. The monomer spacing for vinyl monomers in a polymer is 2.56 Å. The length of a glucose unit in a polysaccharide is 5.15 Å. Regardless of the method of determining the charge spacing, the polyion charge spacing cannot be less than the Bjerrum length because of counterion condensation onto the polymer charges (Manning restriction). If a calculated charge spacing is less than the Bjerrum length, the charge spacing should be set equal to the Bjerrum length.

Data Set **A** – Sodium Carboxymethyl Cellulose

This data is for two sodium carboxymethyl cellulose molecular weight fractions.[73] Experimental information is listed as NaCMC (a) and NaCMC (b) in Table 5. Each fraction had a degree of substitution of 1.06. Intrinsic viscosity measurements were made for each molecular weight fraction over a range of ionic strengths. In Figures 29 and 30 the experimental data is plotted as ~ symbols for NaCMC (a) and **X** symbols for NaCMC (b).

Data Set **B** - Hydrolyzed Polyacrylamide

This data is for three molecular weight polyacrylamides that were hydrolyzed.[74,75] The degree of hydrolysis for each polymer was adjusted over a range from about 5 to 30 %. Experimental information is listed as HPAM (a), HPAM (b) and HPAM (c) in Table 5. As shown in Table 5, the polyion charge spacing decreased as the degree of hydrolysis increased. Intrinsic viscosity measurements were made for each hydrolyzed polyacrylamide at a constant ionic strength of 0.12 moles/liter. In Figures 29 and 30 the experimental data is plotted as symbols for HPAM (a), as **x** symbols for HPAM (b) and as **o** symbols for HPAM (c).

Data Set **C** - Copolymer of Acrylamide and (N,N,N-trimethyl) amionoethyl chloride

This data is for a copolymer containing 70 mole % acrylamide and 30 mole % (N,N,N-trimethyl)amionoethyl chloride.[76] Intrinsic viscosity measurements were made over a range of ionic strengths. Experimental information is listed as AM-CAM in Table 5, and in Figures 29 and 30 the experimental data is plotted as **+** symbols.

Data Set **D** – Partially Neutralized Poly(acrylic acid)

This data is for a 50% ionized poly(acrylic acid).[77] Intrinsic viscosity measurements were made over a range of ionic strengths. Experimental information is listed as PAA in Table 5, and in Figures 29 and 30 the experimental data is plotted as ◊ symbols. Because of the Manning restriction, the polyion charge spacing was set to 7.22 Å, the Bjerrum length of water at 303 K.

Application of Experimental Data to the Modified OSF Theory

As suggested by Equation (12), plots of each data set, expressed as $\eta_{intr}^{2/3}$ vs. L_{screen} / b, are shown in Figure 29. Each data set on this plot was fitted by a straight line. The intercept of each line was considered as the intrinsic viscosity in the absence of electrostatic effects to the 2/3 power, $\eta_{intrHS}^{2/3}$ for the data set. The η_{intrHS} values determined from the intercepts are listed in Table 5.

After the η_{intrHS} values were determined, all the data from the four data sets were then plotted as suggested by Equation (13). This plot is shown as Figure (30). Figure (30a) is a linear plot of $\{(\eta_{intr}^2 - \eta_{intrHS}^2) / M\}^{1/3}$ m_o / l_m vs. L_{screen} / b. Figure (30b), a log-log plot of $\{(\eta_{intr}^2 - \eta_{intrHS}^2) / M\}^{1/3}$ m_o / l_m vs. L_{screen} / b, shows an improved view of the data, especially at the lower abscissa and ordinate values.

Table 5: Experimental Information

Parameter	Polelectrolyte System													
	Data Set A				Data set B						Data Set C		Data Set D	
	NaCMC (a)		NaCMC (b)		HPAM (a)		HPAM (b)		HPAM (c)		AM-CMA		PAA	
Plot Symbol	~		X				x		o		+		◊	
charge	anionic		anionic		anionic		anionic		anionic		cationic		anionic	
T, K	298		298		303		303		303		298		303	
m_o, g/mole	247		247		71		71		71		97.1		71.5	
l_m, Å	5.15		5.15		2.56		2.56		2.56		2.56		2.56	
b, Å	11.0		11.0		See Below		See Below		See Below		11.4		7.22	
I, mole/liter	See Below		See Below		0.12		0.12		0.12		See Below		See Below	
M x 10^{-6} g/mole	1.06		0.75		0.156		0.382		1.14		1.44		0.48	
η_{intrHS}, dL/g	8.83		7.03		0.48		0.95		2.71		2.35		0.24	
	I, mole/liter	**η_{intr}, dL/g**	**I, mole/liter**	**η_{intr}, dL/g**	**b, Å**	**η_{intr}, dL/g**	**b, Å**	**η_{intr}, dL/g**	**b, Å**	**η_{intr}, dL/g**	**I, mole/liter**	**η_{intr}, dL/g**	**I, mole/liter**	**η_{intr}, dL/g**
	0.20	11.75	0.20	9.45	35	0.86	35	1.5	35	4.2	2.10	3.18	1.05	0.45
	0.05	16.3	0.05	12.1	19	1.10	19	2.0	19	5.5	0.89	3.58	0.52	0.60
	0.01	27.0	0.01	19.6	15	1.33	15	2.5	15	6.8	0.50	3.86	0.33	0.72
	0.005	34.8	0.005	25.8	13.5	1.56	12	2.73	12	7.5	0.25	4.60	0.25	0.81
											0.10	6.25	0.10	1.08
											0.05	8.41	0.05	1.70
											0.025	11.19		
											0.015	14.49		
											0.010	18.17		

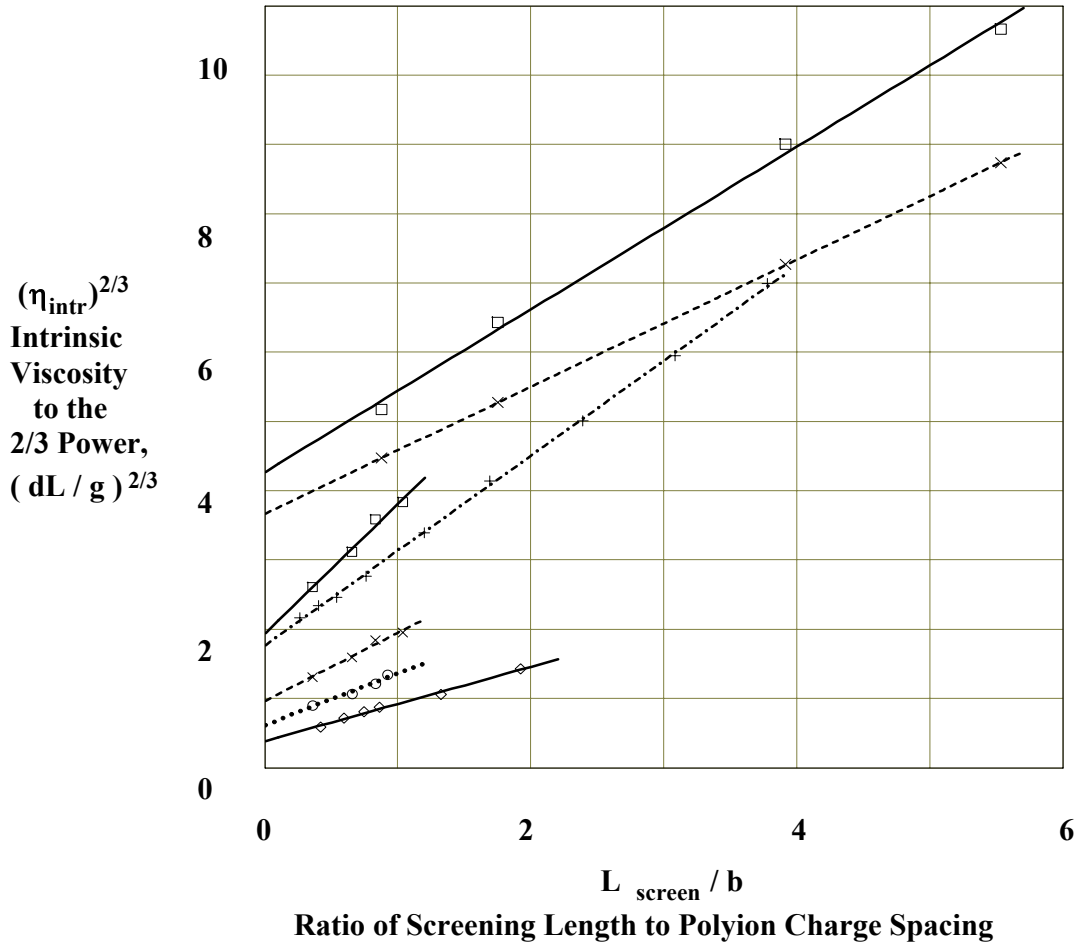

Figure 29: Plot of Experimental Data as Suggested by Equation (12). See Table 5 for Symbol Identification.

Results from Data Analysis Using the Modified OSF Theory

As shown by Figure 30, within expected experimental error, the data forms a straight line as expected from Equation (13). Thus, the modified OSF theory used to develop Equation (13) appears to be consistent with the experimental intrinsic viscosity measurements made using solutions of flexible coil polyelectrolyte solutes in solvents containing a range of sodium chloride salt concentrations.

The slope of the straight line fitted to the data plotted in Figure 30b has a value of 1.06. Because this value is very close to unity, the use of the ratio of screening length to charge spacing to a power of one was appropriate in defining the electrostatic persistence length as expressed by Equation (11).

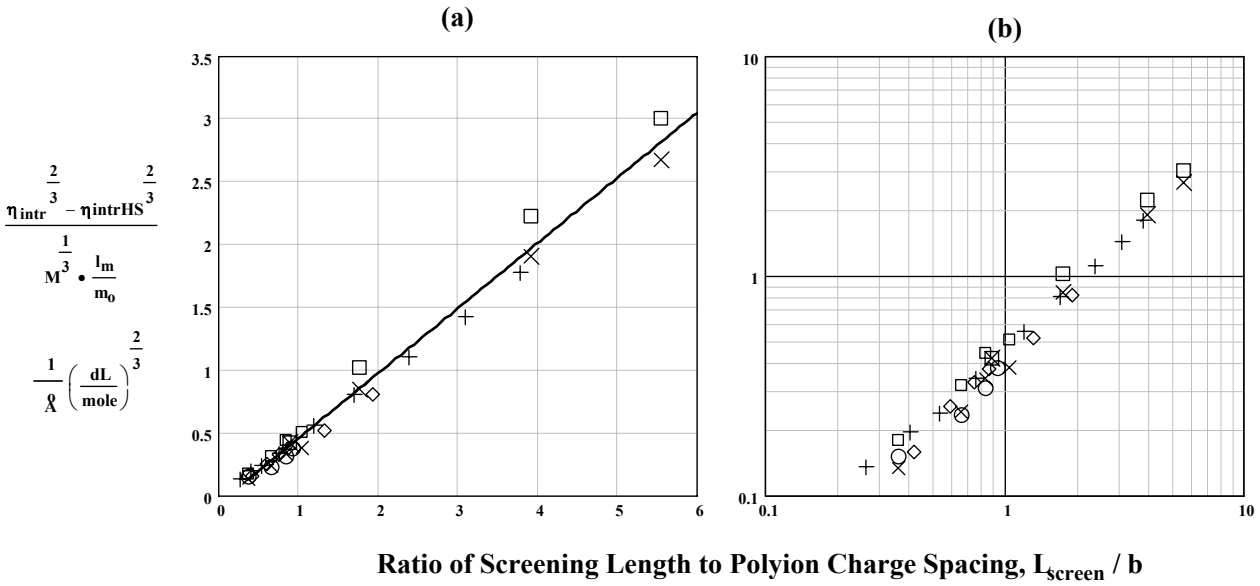

Figure 30: Plot of All Experimental Data as Suggested by Equation (13). (a) linear-linear data plot. (b) log-log data plot. See Table 5 for Symbol Identification.

The slope of the straight line fitted to the data plotted in Figure 30a has a value of 0.518 $(dL/mole)^{2/3}/$ Å. As shown by Equation (13), this slope is equal to k l_B $(\Phi o)^{2/3}$ / 2. Because the constants l_B and Φo are known, the value for k can be calculated from the slope to be 7.19. It was expected that k should have a value close to unity. The high value for k could be attributed to the use of an erroneous value for the dielectric strength of the aqueous medium surrounding the polyion charges. The relative permittivity for the medium surrounding the polyion charges was assumed to be that of bulk water, 78.5. However, if the effective relative permittivity for the medium surrounding the polyion charges is set to1.5, the value for k would be unity. Some rational is needed to justify such a low value for the medium's relative permittivity or equivalently the low value for the effective dielectric constant.

The value of the effective medium dielectric constant, which governs the interaction between polyion charges, is difficult to establish. The effective dielectric constant is expected to be lower than the bulk dielectric constant of water for two reasons.[78] First, the electrical lines of force between two closely spaced ionic charges will tend to pass through the polymer backbone that is organic or hydrocarbon like. Organic molecules such as cyclohexane, pentane and benzene, have relative permittivities that range from 1.8 to 2.3, values much less than water. Secondly, the ions in the charge field surrounding the polyion charges will alter the polarizability of the water molecules in the vicinity of the polyion charges, and thereby lower the medium's dielectric strength. Smaller ion sizes reduce the medium's effective dielectric constant more than larger ions.[79] Positive ions are smaller than negative ions and therefore will reduce the medium's effective dielectric constant more than negative ions. Because of the above discussion, it is not unreasonable that the effective dielectric strength of the medium in the vicinity of polyion charges could be considerably less than that of bulk water.

Oil Recovery Utilitization of Polyelectrolytes

With current enhanced oil recovery methods, the harsh underground environment is detrimental to polymer solution performance. An improved polymer solution would take advantage of reservoir conditions. Our research suggests that for an aqueous polymer solution to be efficient as an oil recovery agent, the polymer molecules should have a small, collapsed conformation near the injection well, and later expand or swell to form large coils upon reaching the porous, petroleum-containing rock formations away from the injection well. The solution environment in underground reservoirs is characterized by high temperature, basic pH, and the presence of monovalent and divalent ions. The conditions of the polymer solution introduced into the injection well, however, can be controlled to some degree. Polyelectrolytes that expand or collapse with changes in the solution environment can be readily synthesized. Therefore, optimization of polymer enhanced oil recovery will most likely result from a combination of a well-designed responsive polymer with a sensible injection technique.

Future Polyelectrolyte Studies

Current work in our laboratories includes the synthesis of a series of polyelectrolyte copolymers having controlled spacing between charges along the polyion backbone. The charge spacing will be incremented according to an experimental design. Intrinsic viscosity studies will then be conducted at appropriate conditions to ensure constant ionic strength, flexible polymer coils, and dilute conditions for reasons explained in this report. These carefully controlled experiments will help to test the validity of the theory herein described, and also to further elucidate the mechanisms through which electrostatic interactions influence polyelectrolyte solution properties. Additionally, extensional viscosities of the polymer solutions will be measured under various solution conditions designed to simulate porous media flow in reservoir environments. It is anticipated that a better understanding of polyelectrolyte solution behavior will lead to the design of an inexpensive polyion that, when injected under proper conditions, will improve petroleum sweep efficiency by responding favorably to environmental changes.

Conclusion

Findings presented in this report will facilitate the design of new polyelectrolytes for improved sweep efficiency during polymer flooding. The scaling theory of polyelectrolyte solutions was found to be useful for determining the acceptable experimental conditions for obtaining valid solution intrinsic viscosities. The treatment of the modified OSF theory presented in this report correlates macromolecular structure and solvent character with solution viscous properties. Although the theory sufficiently describes the solvent-polymer systems for which data has been analyzed, additional systems need to be investigated. It appears that the effective dielectric strength near the polymer chain may be much lower than that of the bulk solution, but quantification of the local dielectric strength has not yet been achieved.

Nomenclature

Symbol	Dimension	Description
b	Å	Average distance between polyion charges
C_p	g / dL	Polymer mass concentration
$C_{polymer}$	mole / liter	Polymer molar concentration
C_{pStar}	mole / liter	Polymer concentration at the overlap condition
C_{salt}	mole / liter	Molar concentration of salt
C_{sMin}	mole / liter	Minimum salt concentration to assure a flexible polymer coil
D	coul^2 / (Newton meter^2)	Dielectric constant, $D = 4 \pi \varepsilon_r \varepsilon_o$
elec	Newton	Charge of an electron, 1.602 x 10^{-19} coul
F	dynes	Electrostatic force between charges
I	mole / liter	Solution ionic strength
k	dimensionless	Constant of proportionality
k_B	erg / K	Boltzmann's constant, 1.380 x 10^{-16} erg per K
L_{screen}	Å	Debye-Hückel screening length
l_B	Å	Bjerrum length
l_m	Å	Monomer length
M	g / mole	Polymer molecular weight
m_o	g / mole	Monomer molecular weight
N_A	1/mole	Avogadro's number, 6.02 x 10^{23} per mole
Q	coul	Charge of an ion
Q'	coul	Charge of an ion
q	Å	Total persistence length
q_e	Å	Persistence length due to electrostatic forces
q_o	Å	Persistence length in the absence of electrostatic forces
s	meters	Distance between charges
T	^{o}K	Absolute temperature
t	^{o}C	Temperature
Z_p	dimensionless	Number of charges on a single polyion
z_i	dimensionless	Charge valence of salt ion i
z_p	dimensionless	Charge valence of the polymer counterions
ε	coul^2 / (Newton meter^2)	Dielectric strength, $\varepsilon = \varepsilon_r \varepsilon_o$
ε_o	coul^2 / (Newton meter^2)	Permittivity of a vacuum, 8.85 x 10^{-12} coul^2 / (Newton meter^2)
ε_r	dimensionless	Relative permittivity
η_o	poise	Solvent viscosity
η_s	poise	Solution viscosity
η_{intr}	dL/g	Polymer solution intrinsic viscosity
η_{intrHS}	dL/g	Polymer solution intrinsic viscosity in absence of electrostatic forces
η_{red}	dL/g	Solution reduced viscosity
Φ_o	1/mole	Flory constant for flexible, polymer coils, 2.86 x 10^{23} /mole
ξ	dimensionless	Manning parameter, $\xi = l_B / b$.

References

[1] Lowe, A. B. and McCormick, C. L. *Chem. Rev.* **2002**, *102*(11), 4177-4189.
[2] Morawetz, H. *Macromolecules in Solution, 2nd Ed*. Robert E. Krieger Publishing Co.: Malabar, FL, 1983, p. 315.
[3] Bekturov, E. A.; Kudaibergenov, S. E.; Rafikov, S. R. *Macromol. Chem. Phys*. **1990**, *C30*, 233.
[4] Candau, F. Regalado, E. J.; Selb E. J., *Macromol. Sym.* **2000**, *150*, 241-249.
[5] McCormick, C. L.; Middleton, J. C.; and Grady, C. E. *Polymer* **1992**, *33*, 4184.
[6] Middleton, J. C. *Ph.D. Dissertation*, University of Southern Mississippi, 1990.
[7] Branham, K. D. *Ph.D. Dissertation*, University of Southern Mississippi, 1995.
[8] Branham, K. D.; Snowden, H. S.; McCormick, C. L. *Macromolecules* **1996**, *29*, 254.
[9] Smith, G. L. and McCormick, C. L. *Macromolecules* **2001**, *34*, 918.
[10] Smith, G. L. and McCormick, C. L. *Macromolecules* **2001**, *34*, 5579.
[11] Smith, G. L. and McCormick, C. L. *Langmuir* **2001**, *17*, 1719.
[12] Kujawa, P.; Rosiak, J. M.; Selb, J.; Candau, F. *Macromol. Chem. Phys.* **2001**, *202*, 1384.
[13] Miyazawa, K. and Winnik, F. M. *Macromolecules* **2002**, *35*, 2440.
[14] Miyazawa, K. and Winnik, F. M. *Macromolecules* **ref?**
[15] Iliopoulos, I.; Wang, T. K.; Audebert, R. *Langmuir* **1991**, *7*, 617.
[16] Kevelam, J.; van Breemen, J. F. L.; Blokzijl, W.; Engberts, J. B. F. N. *Langmuir* **1996**, *12*, 4709.
[17] Mangy, B.; Iliopoulos, I.; Zana, R.; Audebert, R *Langmuir* **1994**, *10*, 3180.
[18] Mangy, B.; Iliopoulos, I.; Zana, R.; Audebert, R. *Langmuir* **1996**, *12*, 2616.
[19] Magny, B.; Iliopoulos, I.; Audebert, R.; Piculell, L; Lindman, B. *Prog. Colloid Polym. Sci.* **1992**, *89*, 118.
[20] Schwuger, M. J. *J. Colloid Interface Sci.* **1973**, *43*, 491.
[21] Arai, H.; Murata, M.; Shinoda, K. *J. Colloid Interface Sci.* **1971**, *37*, 223.
[22] Francois, J.; Dayantis, J.; Sabbadin, J. *Eur. Polym. J.* **1985**, *21*,1965.
[23] Zana, R.; Lang, J.; Lianos, P. *Polym. Prepr. Am. Chem. Soc. Div. Polym. Chem.* **1982**, *23*, 39.
[24] Brackman, J. C.; Engberts, J. B. F. N. *Langmuir* **1992**, *8*, 424.
[25] Brackman, J. C.; Engberts, J. B. F. N. *Chem. Soc. Rev.* **1993**, *22*, 85.
[26] Leontidis, E.; Kyprianidou-Leodidou, T.; Caseri,, W.; Kyriacou, K. *Langmuir* **1999**, *15*, 3381.
[27] Purcell, I. P.; Thomas, R. K.; Penfold, J.; Howe, A. M. *Colloids and Surfaces* **1995** *94*, 125.
[28] Ghosh, S.; Moulik, S. P. *Indian Journal of Chemistry* **1999**, *38*, 10.
[29] Goddard, E. D.; Phillips, T. S.; Hannan, R. B. *J. Soc. Cosmet. Chem*. **1975**, *26*, 461.
[30] Goddard, E. D.; Hannan, R. B. *J. Am. Oil Chem. Soc.* **1977**, *54*, 561.
[31] Cockbain, E. G. *Trans. Faraday Soc.* **1953**, *49*, 104.
[32] Hayakawa, K.; Kwak, J. C. T. *J. Phys. Chem.* **1982**, *86*, 3866.
[33] Santerre, J. P.; Hayakawa, K.; Kwak, J. C. T. *Colloids Surfaces* **1985**, *13*, 35.
[34] Asnacios, A.; Langeven, D.; Argillier, J. F. *Eur. Phys. J. B* **1998**, *5*, 905.
[35] Asnacios, A.; Langevin, D.; Argillier, J. F. *Macromolecules* **1996**, *29*, 7412.
[36] Bekturov, E. A.; Kudaibergenov, S. E.; Kanapyanova, G. S. *Polym. Bull*. **1984**, *11*, 551.
[37] Harrison, I. M.; Candau, F.; Zana, R. *Col. Polym. Sci.* **1999**, 277(1), 48-57.
[38] McCormick, C. L.and Salazar, L. C. *Polymer* **1992**, *33*(21), 4617-24.
[39] Kathmann, E. E.; White, L. A.; McCormick, C. L. *Polymer* **1997**, *38*(4), 871-878.
[40] Biggs, S.; Hill, A.; Selb, J. Candau, F. *J. Phys. Chem.* **1992**, *96*, 1505.
[41] Ezzell, S. A.; Hoyle, C. E.; Creed, D.; McCormick, C. L. *Macromolecules* **1992**, *25*, 1881.
[42] Ezzell, S. A.; Hoyle, C. E.; Creed, D.; McCormick, C. L. *Macromolecules* **1992**, *25*, 1887.
[43] Peiffer, D. G.; Lundberg, R. D. *Polymer* **1985**, *26*, 1058.
[44] Laughlin, R. G. In *Advances in Liquid Crystals, Vol. 3*; Brown G. H., Ed.; Academic Press: New York, **1979**, p. 41 and 99.
[45] Laughlin, R. G. *Langmuir*, **1991**, *7*, 842.
[46] Kathmann, E. E.; McCormick, C. L. *J. Polym. Sci. Part A* **1997**, *35*, 231.
[47] Guillemet, F.; Piculell, L.; Nilsson, S.; Djabourov, M.; Lindman, B. *Progr. Colloid Polym. Sci.* **1995**, *98*, 47.
[48] Loyen, K.; Iloiopoulos, I.; Olsson, U.; Audebert, R. *Progr. Colloid Polym. Sci*. **1995**, *98*, 42.
[49] Iliopoulos, I.; Olsson, U. *J. Phys. Chem.* **1994**, *98*, 1500.
[50] Pisarik, M.; Bako, D. *Acta Polymer.* **1994**, *45*, 93.
[51] Panmai, S.; Prud'homme, R. K.; Peiffer, D. G. *Coll. Surf., A: Physicochem. Eng. Aspects*, **1999**, *147*, 3.

[52] Nishikawa, K.; Yekta, A.; Pham, H. H.; Winnik, M. A.; Sau, A. C. *Langmuir* **1998**, *14*, 7119.
[53] Goddard, E. D. In *Interactions of Surfactants with Polymers and Proteins*, Goddard, E. D. and Ananthapadmanabhan, Eds. CRC Press: Boca Raton, FL, 1993, pp 123-201.
[54] Rajagopalan, V.; Olsson, U.; Iliopoulos, I. *Langmuir* **1996**,*12*, 4378.
[55] Bagger-Jorgensen, J.; Olsson, U.; Iliopoulos, I. *Langmuir* **1995**, *11*, 1934.
[56] Jones, M. N. *J. Coll. Interface Sci*. **1967**, *23*, 36.
[57] Bergeron, V.; Langevin, D.; Asnacios, A. *Langmuir,* **1996**, *12*, 1550.
[58] W. M. Thomas, and D. W. Wang, in *Encycl. Polym. Sci. Eng, Second Ed.* H. F. Mark, N. M. Bikales, C. G. Overberger, G. Menges, J. I. Kroschwitz, Eds., Vol. 1, Wiley Interscience, New York, 1985, pp 176-177.
[59] Semi-Annual Report, Stimuli Responsive Polymers, DOE DE-FC26-01BC15317.
[60] Mark, F.; *et al*., *Encyclopedia of Polymer Science and Engineering, Volume 11*, John Wiley & Sons: New York, 1964.
[61] Lange, N. A.; Forker; G. M. Eds., *Handbook of Chemistry*, McGraw-Hill Book Company, Inc.: New York, 1956.
[62] Manning, G. S.; *The Journal of Chemical Physics* **1969**, *51*, 924.
[63] Dobrynin A.; Colby, R. H.; Rubinstein, M.; *Macromolecules* **1995**, *28*, 1-45.
[64] Barrat, J.-L.; Joanny, J.-F.; *Europhysics Letters* **1993**, *24*, 333-338.
[65] DeGennes, P.G.; Pincus, P.; Velasco, R. M.; Brochard, F.; *Journal de Physique (Paris)* **1976**, *37*, 1461.
[66] Skolnick, J.; Fixman, M.; *Macromolecules* **1997**, *10*, 944-948.
[67] Odijk, T.; *Macromolecules* **1979**, *12*, 688-693.
[68] Yamakawa, A.; Fujii, M.; *Macromolecules* **1974**, *7*, 128-135.
[69] Tobitani, A.; Ross-Murphy, S. B.; *Polymer International* **1997**, *44*, 338-347.
[70] Takahashi, A.; Nagasawa, M.; *JACS* **1964**, *86*, 543-548.
[71] Tricot, M.; *Macromolecules*, **1984**, *17*, 1698-1704.
[72] Reed, W. F.; Ghosh, S.; Medjahdi, G.; Francois, J.; *Macromolecules* **1991**, *24*, 6189-6198.
[73] Brown, W.; Henley, D.; *Makromol. Chem.* **1964**, *79*, 68-88.
[74] Kulkarni, R. A.; Gundiah, S.; *Makromol. Chem.* **1984**, *185*, 957-967.
[75] Kulkarni, R. A.; Gundiah, S.; *Makromol. Chem.* **1984**, *185*, 969-982.
[76] Mabire, F.; Audebert, R.; Quivoron, C.; *Polymer* **1984**, *25*, 1317-1322.
[77] Mylonas, Y.; Staikos, G.; Ullner, M.; *Polymer* **1999**, *40*, 6841-6847.
[78] Tanford, C.; *Physical Chemistry of Macromolecules,* John Wiley & Sons, Inc.: New York, 1961.
[79] Berry, R. S.; Rice, S. A.; Ross, J.; Eds.; *Physical Chemistry, 2nd Ed.*; Oxford University Press: New York, 2000.